The Paleocene-Eocene benthic foraminiferal extinction and stable isotope anomalies

E. Thomas and N. J. Shackleton

Email alerting service	click here to receive free e-mail alerts when new articles cite this article
Permission request	click here to seek permission to re-use all or part of this article
Subscribe	click here to subscribe to Geological Society, London, Special Publications or the Lyell Collection

Notes

Lyell Collection

The Paleocene–Eocene benthic foraminiferal extinction and stable isotope anomalies

E. THOMAS[1,2] & N. J. SHACKLETON[3]

[1] Department of Earth Sciences, Downing Street, University of Cambridge,
Cambridge CB2 3EQ, UK
Present address: Center for the Study of Global Change, Department of Geology
and Geophysics, PO Box 208109, Yale University, New Haven CT 06520-8109, USA
[2] Department of Earth and Environmental Sciences, Wesleyan University,
Middletown, CT 06459-1309, USA
[3] Godwin Laboratory, Subdepartment of Quaternary Research, University of Cambridge,
Cambridge CB2 3RS, UK

Abstract: In the late Paleocene to early Eocene, deep sea benthic foraminifera suffered their only global extinction of the last 75 million years and diversity decreased worldwide by 30–50% in a few thousand years. At Maud Rise (Weddell Sea, Antarctica; Sites 689 and 690, palaeodepths 1100 m and 1900 m) and Walvis Ridge (Southeastern Atlantic, Sites 525 and 527, palaeodepths 1600 m and 3400 m) post-extinction faunas were low-diversity and high-dominance, but the dominant species differed by geographical location. At Maud Rise, post-extinction faunas were dominated by small, biserial and triserial species, while the large, thick-walled, long-lived deep sea species *Nuttallides truempyi* was absent. At Walvis Ridge, by contrast, they were dominated by long-lived species such as *N. truempyi*, with common to abundant small abyssaminid species. The faunal dominance patterns at the two locations thus suggest different post-extinction seafloor environments: increased flux of organic matter and possibly decreased oxygen levels at Maud Rise, decreased flux at Walvis Ridge. The species-richness remained very low for about 50 000 years, then gradually increased.

The extinction was synchronous with a large, negative, short-term excursion of carbon and oxygen isotopes in planktonic and benthic foraminifera and bulk carbonate. The isotope excursions reached peak negative values in a few thousand years and values returned to pre-excursion levels in about 50 000 years. The carbon isotope excursion was about –2‰ for benthic foraminifera at Walvis Ridge and Maud Rise, and about –4‰ for planktonic foraminifera at Maud Rise. At the latter sites vertical gradients thus decreased, possibly at least partially as a result of upwelling. The oxygen isotope excursion was about –1.5‰ for benthic foraminifera at Walvis Ridge and Maud Rise, –1‰ for planktonic foraminifera at Maud Rise.

The rapid oxygen isotope excursion at a time when polar ice-sheets were absent or insignificant can be explained by an increase in temperature by 4–6°C of high latitude surface waters and deep waters world wide. The deep ocean temperature increase could have been caused by warming of surface waters at high latitudes and continued formation of the deep waters at these locations, or by a switch from dominant formation of deep waters at high latitudes to formation at lower latitudes. Benthic foraminiferal post-extinction biogeographical patterns favour the latter explanation.

The short-term carbon isotope excursion occurred in deep and surface waters, and in soil concretions and mammal teeth in the continental record. It is associated with increased $CaCO_3$-dissolution over a wide depth range in the oceans, suggesting that a rapid transfer of isotopically light carbon from lithosphere or biosphere into the ocean–atmosphere system may have been involved. The rapidity of the initiation of the excursion (a few thousand years) and its short duration (50 000 years) suggest that such a transfer was probably not caused by changes in the ratio of organic carbon to carbonate deposition or erosion. Transfer of carbon from the terrestrial biosphere was probably not the cause, because it would require a much larger biosphere destruction than at the end of the Cretaceous, in conflict with the fossil record. It is difficult to explain the large shift by rapid emission into the atmosphere of volcanogenic CO_2, although huge subaerial plateau basalt eruptions occurred at the time in the northern Atlantic. Probably a complex combination of processes and feedback was involved, including volcanogenic emission of CO_2, changing circulation patterns, changing productivity in the oceans and possibly on land, and changes in the relative size of the oceanic and atmospheric carbon reservoirs.

During the late Paleocene and early Eocene important changes occurred in global climate, in plate tectonic processes and in the global carbon cycle. The discussion of these events has been complicated and confused by two facts: that there is no unequivocal definition of the 'Paleocene–Eocene boundary' because these words mean different things to different people (e.g. Berggren & Aubry 1996); and that different events occurred at different time scales, from millions of years to thousands of years. We will first discuss longer timescale events, occurring over several millions of years in palaeomagnetic chrons C25 and C24, at about 55–60 Ma in the geo-magnetic polarity time scale of Berggren et al. (1985), and 52.5–57.5 Ma in that of Cande & Kent (1995). The beginning of this interval has generally been placed in the Paleocene and the end in the Eocene, but the location of the boundary has varied.

This transitional Paleocene–Eocene period witnessed a long-time warming of the deep oceans beginning in the earliest Paleocene, and a long-term decrease of carbon isotopic values in tests of benthic and planktonic foraminifera and bulk carbonate, beginning in early Chron C25 (Shackleton 1986, 1987; Zachos et al. 1993). High-latitude areas experienced the highest temperatures of the Cenozoic as indicated by the presence of warm-water pelagic marine organisms (e.g. Haq et al. 1977; Premoli-Silva & Boersma 1984; Boersma et al. 1987; Stott & Kennett 1990; Aubry 1992; Berggren 1992; Ottens & Nederbragt 1992). Crocodiles, turtles and other thermophilic biota occurred at high northern latitudes (Estes & Hutchison 1980; McKenna 1980; Gingerich 1983; Markwick 1994) in the presence of vegetation and soil-types indicating warm climates (Kemp 1978; Nilsen & Kerr 1978; Wolfe 1978; Wolfe & Poore 1982; Schmidt 1991). Palynological data from the North Sea indicate peak warmth (Schroeder 1992). Clay mineral associations in oceanic sediments indicate high humidity and intense chemical weathering as indicated by high abundances of kaolinite (Robert & Maillot 1990; Robert & Chamley 1991; Robert & Kennett 1992, 1994); similar peaks in kaolinite abundance have been observed in sediments from the New Jersey margin (Gibson et al. 1993) and the North Sea region (Knox, written comm. 1993). Oxygen isotopic measurements show high temperatures and shallow temperature gradients from low to high latitudes (Shackleton & Boersma 1981; Oberhänsli & Hsü 1986; Stott et al. 1990; Barrera & Huber 1991; Seto et al. 1991; Stott 1992; Zachos et al. 1994; Bralower et al. 1995a, b). Dust concentrations in oceanic sediments reached very low levels in the upper part of Chron C24r (Janecek & Rea 1983;

Miller et al. 1987b; Rea et al. 1990; Hovan & Rea 1992; Rea 1994), suggesting very low wind strength.

During this warm period terrestrial and shallow-water marine organisms did not suffer major net extinctions (e.g. Raup & Sepkoski 1986), but it was a time of major origination of species and high diversity on land (European mammals and flora: Hooker 1991; Collinson 1983; North American mammals: Butler et al. 1981, 1987; Wing 1984; Rea et al. 1990; Wing et al. 1991) and in the surface oceans (e.g. planktonic foraminifera: Kennett 1978; Boersma et al. 1987; Boersma & Premoli-Silva 1991; Corfield & Shackleton 1988; Berggren 1992; Corfield 1993; calcareous nannofossils: Romein 1979; Aubry 1992; dinoflagellates, Oberhänsli & Hsü 1986; McGowran 1991).

An explanation of the several million year-long warm period has commonly been sought in elevated levels of atmospheric CO_2, caused by plate tectonic related processes (e.g. Williams 1986; McGowran 1991; Rea et al. 1990). During Chrons C24–C25 there was a worldwide plate-tectonic reorganization, involving the slow-down of the northward motion of the Indian subcontinent because of its collision with Asia (Klootwijk et al. 1991; Beck et al. 1995a). According to some researchers high-temperature metamorphism started in the Himalayas (Tonarini et al. 1993; Smith et al. 1994; Beck et al. 1995a) and delivered large amounts of CO_2 to the atmosphere by decarbonation (Touret 1992; Kerrick & Caldeira 1993, 1994), but this mechanism of CO_2 delivery has been doubted (Selverstone & Gutzler 1993). Increasing levels of CO_2 in the atmosphere resulting from the India–Asia collision could alternatively have been generated by erosion of sediments rich in organic matter (Beck et al. 1995b). In addition, subduction changed in direction in the North Pacific (Goldfarb et al. 1991). Continental break-up started in the North Atlantic (Roberts et al. 1984; Eldholm 1990; Larsen et al. 1992), accompanied by violent, partially subaerial plateau basalt eruptive activity (White 1989; White & MacKenzie 1989; Eldholm & Thomas 1993; Kaiho & Saito 1994). High hydro-thermal activity along Pacific oceanic ridges may have contributed to increased atmospheric CO_2 levels (Owen & Rea 1985; Olivarez & Owen 1989; Kyte et al. 1993), although it is doubted whether increased spreading activity will cause a net increase in atmospheric pCO_2 (Staudigel et al. 1989; Varekamp et al. 1992). High concentrations of other greenhouse gases such as methane have also been invoked (Sloan et al. 1992, 1995).

High atmospheric pCO_2 can not fully explain the global climate, however: how could high latitudes have warmed while the equatorial regions were not

warmer than today (Shackleton & Boersma 1981; Zachos *et al.* 1994; Sloan *et al.* 1995)? The oceans could have transported more heat, involving a larger part of the ocean waters (Barron 1987; Sloan & Barron 1992; Barron & Peterson 1991), but it is not clear that even involvement of the whole ocean in heat transport can succeed in keeping the high latitudes at the temperatures of 15–18°C suggested by oxygen isotope studies (Crowley 1991; Walker & Sloan 1992; Sloan *et al.* 1995). The theory of increased oceanic heat transport appeared attractive because it had been long theorized that deep and intermediate waters in the oceans could have formed as high salinity, high temperature waters by evaporation in subtropical latitudes in the absence of very cold polar areas (Chamberlin 1906; Brass *et al.* 1982; Hay 1989). Surface oceans at low latitudes show the cooling expected if heat transport was more active than today (Zachos *et al.* 1993, 1994; Bralower *et al.* 1995*b*). The mechanisms for enhanced oceanic heat transport, however, remain undefined (Sloan *et al.* 1995).

Evidence for the presence of such warm saline bottom water (WSBW) is not unequivocal. Some investigators suggest that WSBW was the dominant water mass over much of the Cenozoic (Matthews & Poore 1980; Prentice & Matthews 1988), or during at least the early Paleogene (Kennett & Stott 1990). Some models, however, predict that the deep oceans will turn anoxic over large regions when deep waters form largely at subtropical latitudes (Herbert & Sarmiento 1991), and this did not happen during the Cenozoic (e.g. Thomas 1992). Some investigators concluded that much of the oceans' intermediate and deep waters was formed at high southern latitudes during most of the Maastrichtian and Cenozoic (e.g. Barrera *et al.* 1987; Miller *et al.* 1987*a*; Katz & Miller 1991; Thomas 1992; Zachos *et al.* 1992, 1993).

Major changes in the deep-water environments of the oceans would be expected to result from a reversal in deep water circulation (Kennett & Stott 1991), and these should be reflected in the composition of deep-sea benthic foraminiferal faunas. Paleocene deep-sea benthic foraminiferal faunas closely resemble Late Cretaceous faunas (Cushman 1946), and the major break in deep-sea benthic foraminiferal faunas occurred somewhere in Chron 24, i.e. between Paleocene and Eocene if seen at coarse time-scales (e.g. Beckmann 1960; von Hillebrandt 1962; Braga *et al.* 1975; Schnitker 1979; Tjalsma & Lohmann 1983; Boersma 1984*b*; Thomas 1990*b*; Bolli *et al.* 1994). In Chron 24r (corresponding to planktonic foraminiferal zones P5–P6, and calcareous nannofossil zone NP9) major faunal change occurred in bathyal and abyssal faunas in all the world's oceans (Miller *et al.* 1987*b*; Boltovskoy & Boltovskoy 1988, 1989;

Berggren & Miller 1989; Thomas 1989, 1990*a, b*, 1992; Katz & Miller 1991; Mackensen & Berggren 1992; Reynolds 1992, unpublished MSc thesis, Univ. of Maine; Pak & Miller 1992, 1995; Nomura 1991; Kaiho 1988, 1991, 1994*a, b*; Miller *et al.* 1992; Kaiho *et al.* 1993; Bolli *et al.* 1994.

Benthic foraminifera underwent coeval extinction in neritic to upper–middle bathyal environments in land sections from Israel to Egypt, North Africa and Spain (Molina *et al.* 1992; Speijer 1994), in the North Sea shelf seas (King 1989; Charnock & Jones 1990), in New Jersey (USA, Gibson *et al.* 1993), and along the western Pacific margin from Japan (Kaiho 1988) to New Zealand (Hornibrook *et al.* 1989; Kaiho *et al.* 1993). At these depths the faunal change was associated with low oxygen conditions, as indicated by the presence of black or dark grey, commonly laminated sediments (North Sea, Japan, New Zealand, New Jersey, Spain, Israel, Egypt). Many authors have explained these conditions as resulting from local lack of circulation (e.g. for the North Sea Basin; Charnock & Jones 1990), but such local effects occurred during worldwide low oxygen conditions, which may have been at least partially responsible.

Some authors suggested that relatively low oxygen conditions also occurred, at least locally, in the world's deep oceans (Thomas 1990*b*, 1992; Kaiho 1991). Most authors implied at least some form of change in deep-water circulation in the benthic foraminiferal extinction, which was seen as caused by changes in temperature as well as nutrient and oxygen content of the deep waters (Miller *et al.* 1987*b*; Thomas 1989; Katz & Miller 1991; Nomura 1991). Others suggested that oceanic productivity decreased drastically (e.g. Moore *et al.* 1984; Shackleton 1987; Shackleton *et al.* 1985; Corfield & Shackleton 1988; Rea *et al.* 1990; Corfield & Cartlidge 1992*a, b*; Corfield 1993), with possible effects on the benthic faunas. Yet others suggested that at least in some areas productivity increased (Thomas 1992; Speijer 1994).

Only recently, however, has it become clear that the deep sea benthic extinction in the latest Paleocene was a unique event in its global extent and rapidity (Thomas 1989; Kennett & Stott 1991; Pak & Miller 1992; Kaiho 1994*b*; Robert & Kennett 1994). In the next paragraphs we will discuss events which happened on timescales of thousands to ten thousands and not millions of years, at some time early in the reversed part of chron C24, in nannofossil zone NP9, and in planktonic foraminiferal zone P5 (Berggren & Aubry 1996; Aubry *et al.* 1996). It had seemed reasonable to suppose that the benthic foraminiferal extinction was not synchronous world wide (Miller *et al.*

1987*b*) because a mechanism for globally synchronous extinction in such a large part of the earth's environment as the deep ocean is difficult to envisage. The observation, however, that the extinction was coeval with a very large, short-term negative excursion in the benthic as well as planktonic d^{13}C and d^{18}O records at ODP Site 690 (Kennett & Stott 1991) suggested that the extinction might have been caused by rapid warming at high latitudes, causing large-scale changes in oceanic circulation and upheaval in the global carbon cycle. Additional research demonstrated that the short-term, extremely negative shift in the carbon isotope values was, as expected by Kennett & Stott (1991), a more than local phenomenon: the event has been recognized in the Bay of Biscay (Pak & Miller 1992; Stott *et al.* 1996), Pacific Ocean (Pak & Miller 1992, 1995; Bralower *et al.* 1995*a, b*), and Indian Ocean (Thomas *et al.* 1992; Lu & Keller 1993). A large negative anomaly in carbon isotopes was also recognized in enamel of land-herbivore teeth and in carbonate concretions, clearly demonstrating that the atmosphere as well as the ocean was involved (Koch *et al.* 1992; Stott *et al.* 1996).

The globally averaged magnitude of the short-term shift is in question: it is about −2‰ in the deep Antarctic (Kennett & Stott 1991; this paper) and the southern Indian Ocean (Lu & Keller 1993), but only about −1‰ in the Pacific and the Bay of Biscay (Pak & Miller 1992). The smaller values may not reflect a global average because the iso-

tope excursion was very short-lived, there may have been hiatuses at Site 577 (Berggren *et al.* 1995), and sampling by Pak & Miller (1992) was not so detailed as to ensure capture of the most extreme values.

The explanation of these short-term changes in climate and in the carbon cycle is being actively debated. Oxygen isotope data suggest rapid warming (over less than 5000 years) of the deep ocean waters at high and low latitudes by 4–6°C, but essentially no warming of surface waters in the tropical Pacific (Zachos *et al.* 1994; Bralower *et al.* 1995*a, b*), so that latitudinal temperature gradients of surface water were very low for about 50 000 years. Such a rapid, deep ocean-wide temperature change has been explained by a change in dominant oceanic circulation pattern, from dominant production of deep to intermediate waters at high latitudes to dominant production in subtropical regions (e.g. Kennett & Stott 1991; Thomas 1992). Major questions remain as to the exact nature of the upheaval in the carbon cycle, the feedback processes resulting from atmosphere–ocean interactions, and whether deep to intermediate waters did indeed form dominantly at subtropical latitudes, and for how long? In this paper, we present new benthic faunal and isotope data at high resolution from four sites at different depths in the southeastern Atlantic Ocean and the Weddell Sea (Fig. 1), to investigate the magnitude of the isotopic excursions in different areas and at different water depths. We use the new, detailed data to discuss
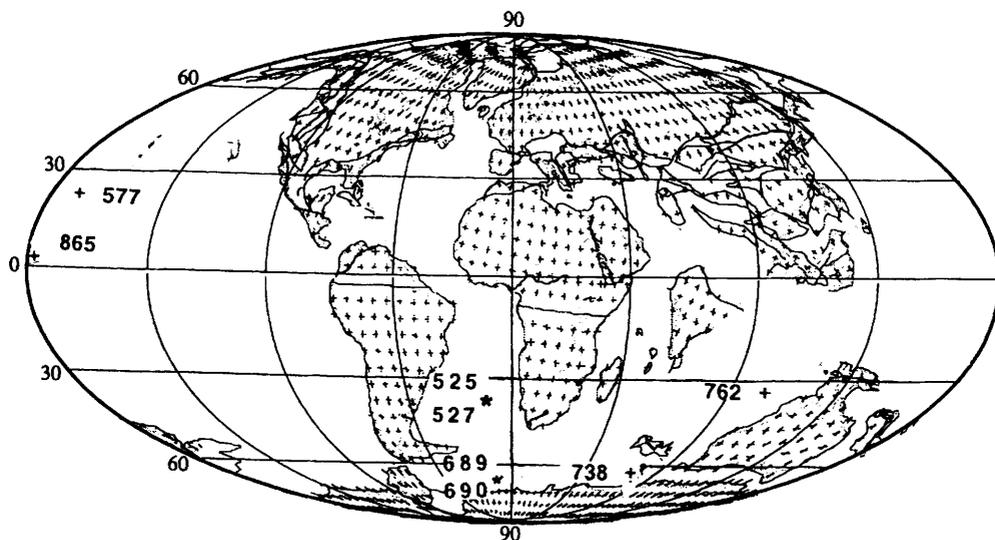
Fig. 1. Palaeogeographic map of the continents in the late Paleocene, after Zachos *et al.* (1994). Sites from which data are presented in this study are indicated by *; other sites mentioned in the text by +.

the bathymetric and biogeographical patterns of the benthic foraminiferal extinction, and re-evaluate the existing database.

Material and methods

Sites and stratigraphy: Maud Rise

Sites 689 (64°31.009'S, 03°05.996'E, present water depth 2080 m) and 690 (65°9.629'S, 1°12.296'E, present water depth 2914 m) were drilled on Maud Rise at the eastern end of the Weddell Sea (Barker et al. 1988, fig. 1). Site 689 is on the northeastern side of the ridge near its crest, Site 690 is 116 km to the southwest on its southwestern flank. Depth estimates for the sites at the end of the Paleocene, based on faunal contents, agreed well with back-tracking estimates, giving about 1100 m for Site 689, about 1900 m for Site 690 (Thomas 1990, 1992). At both sites sediments of Maastrichtian to Pleistocene age were recovered. Paleogene bio-magnetostratigraphy was reviewed by Thomas et al. (1990). Upper Paleocene to lower Eocene sediments consist of chalks and calcareous oozes, with admixture of fine-grained terrigenous matter at Site 690. Recovery was good at Site 690, less so at 689. Core deformation was minimal, but the biostratigraphy was difficult to interpret because the high latitude of the sites caused the absence of many marker species of planktonic foraminifera, and opened the possibility of diachroneity for nannofossil markers (Pospichal & Wise 1990; Aubry et al. 1996). Major differences of opinion in the interpretation of the records centred on the lowermost Eocene. Stott & Kennett (1990) maintained that the section was basically complete over the upper Paleocene–lowermost Eocene, whereas Spieß (1990), Thomas et al. (1990) and Pospichal & Wise (1990) thought there was at least one, about 2 million year-long hiatus in Chrons 22 and 23. Aubry et al. (1996) concluded that an additional hiatus occurs in Chron C24n.

We do not agree with Kennett & Stott (1991) that the records at Site 690 were undisturbed by bio-turbation. In our opinion, the sediments show a different ichnofossil assemblage in the interval just after the extinction event, but no lamination. A few corroded specimens of Gavelinella beccariiformis are present two samples above the extinction, and presumably reworked. Therefore we think that the exact sequence of events in samples spaced only by a few centimetres is difficult to determine.

At Site 689 the upper Paleocene–lower Eocene succession was very incomplete, but a section of sediment extending from in the lower part of Core 689B-22X to the poorly recovered Core 689B-24X contains the benthic foraminiferal extinction and the CP7/CP8 nannofossil zonal boundary (Thomas

1990; Pospichal & Wise 1990; Thomas et al. 1990). The section is bounded by hiatuses and sedimentation rates can not be determined with precision.

Benthic foraminifera were studied by Thomas (1990a); in this paper we present additional data at higher resolution for Sites 689 and 690 (Appendices 1, 2). For Site 690 our data are from Cores 690B-16 to 690B-22, encompassing sediment deposited in Chron C24r according to Aubry et al. (1996). Our data from Hole 689B are from the interval described above (Fig. 2). Carbon and oxygen isotope data of benthic foraminifera were collected by Kennett & Stott (1990, 1991), for planktonic foraminifera by Stott et al. (1990) and Corfield & Cartlidge (1992b), and for bulk carbonate by Shackleton & Hall (1990). We present additional data at high resolution for both sites (Appendix 5).

Sites and stratigraphy: Walvis Ridge

Sites 525 (29.°04.24'S, 02°59.12'E, present water depth 2467 m) and 527 (28°02'49'S, 01°45.80'E, present water depth 4428 m) were drilled on the summit area and the lowermost western slopes of the Walvis Ridge, respectively (Moore et al. 1984, fig. 1). At both sites, Paleocene to Eocene calcareous oozes and chalks were recovered (Shackleton et al. 1984a). Palaeodepths for the end of the Paleocene as derived by backtracking (1600 m for Site 525, 3400 m for Site 527; Moore et al. 1984) are in agreement with benthic faunal data (Boersma 1984b; this paper). Carbon and oxygen isotope data from foraminifera as well as bulk carbonate were determined (Shackleton et al. 1984b; Shackleton & Hall 1984). Nannofossil stratigraphy was described at fairly low resolution by Manivit (1984) and in more detail by Backman (1986a, b). Planktonic and benthic foraminiferal biostratigraphy at low resolution was described by Boersma (1984a, b).

In this paper, we present additional benthic faunal data and isotope data on benthic foraminifera and bulk carbonate over the interval of the benthic extinction. At both sites, despite the difference in palaeodepths, the extinction occurred within the lower few centimetres, but above the base of, an interval of dissolution of 40–50 cm thick, with a sharp lower boundary and a gradual upper boundary (Table 1). In this interval plank-tonic foraminifera were fragmented, but benthics showed good preservation. We took samples from the cores in which the extinction occurred only.

Numerical ages

Numerical ages for Paleocene sediments are in the process of being revised (e.g. Odin & Luterbacher
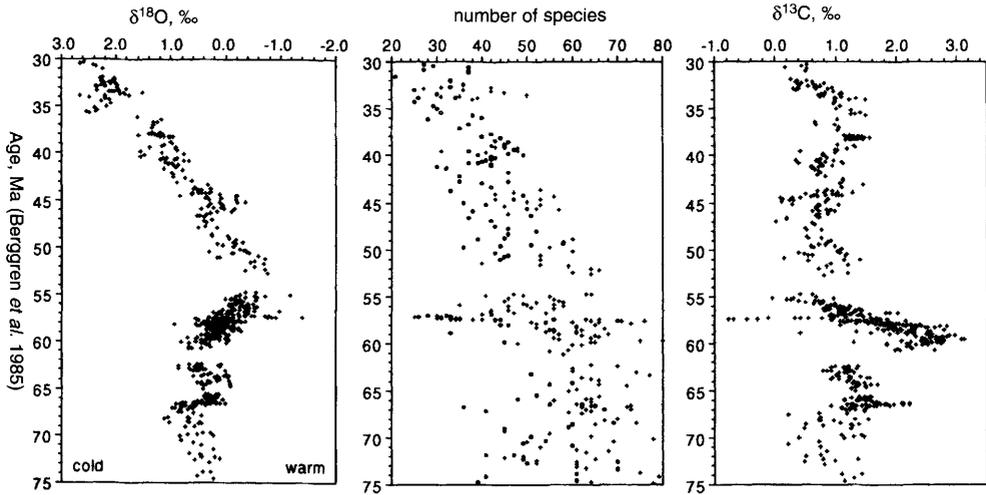
Fig. 2. Benthic foraminiferal carbon and oxygen isotope data (Kennett & Stott 1990; this paper) and species richness of benthic foraminifera (Thomas 1990; this paper) over the Upper Cretaceous through middle Oligocene at Maud Rise, plotted versus numerical age on the Berggren *et al.* (1985) and Aubry *et al.* (1988) timescale. Note the extreme nature of the carbon isotope event as compared to the events at the K/T boundary (66.4 Ma), and its location toward the end of the long-term shift to more negative values, from about 61–58 Ma.

1992) and major changes are proposed from the Berggren *et al.* (1985) and Aubry *et al.* (1988) geomagnetic polarity timescale. The most recent compilations show Paleocene–Eocene boundary ages several million years less than in these two papers (Wing *et al.* 1991; Cande & Kent 1992, 1995; Jenkins & Luterbacher 1992; Odin & Luterbacher 1992; Berggren *et al.* 1995; Berggren & Aubry, 1996; Aubry *et al.* 1996). We are concerned with events during Chron C24r, which has changed little in length between different time scales (around 2.5 million years), although its numerical age has changed from 56.14–58.64 Ma in Berggren *et al.* (1985) to 53.250–55.981 Ma (Cande & Kent 1992) to 53.347–55.904 Ma (Cande & Kent 1994; see also Berggren & Aubry 1996).

Modifications have also been proposed for the planktonic foraminiferal zonation in the Paleocene–Eocene boundary interval (Berggren *et al.* 1995). In the new zonation Zones P5 and P6a of Berggren & Miller (1988) are combined in Zone P5 (the *Morozovella velascoensis* Partial Range Zone; Berggren *et al.* 1995). This revised zonation supports our statement that the benthic foraminiferal extinction was synchronous worldwide. At Sites 525 and 527 the benthic extinction occurred before the last appearance of *Morozovella velascoensis* and before the first appearance of *Morozovella subbotinae* (Boersma 1984a), i.e. in planktonic foraminiferal Zone P5 as modified by Berggren *et al.* (1995). In the planktonic

Table 1. *Dissolution intervals and benthic foraminiferal extinction, Walvis Ridge sites*

	Depth (mbsf)	
	Hole 525A	Hole 527
Top dark layer	391.87–392.01	200.37–200.56
Benthic extinction	392.41–392.57	200.89–201.07
Bottom dark layer	392.57	201.08

foraminiferal zonation of Berggren & Miller (1988) the extinction occurred in Zone P5 at Sites 525 and 527, but in P6a at equatorial Pacific Site 577 (Miller *et al.* 1987*b*; Pak & Miller 1992) and in Mediterranean land sections (Speijer 1994).

We agree with Pak & Miller (1992) and Aubry *et al.* (1996) that the benthic extinction occurs lower in palaeomagnetic Chron C24r than estimated by assuming constant sedimentation rates in Chron 24r (Kennett & Stott 1991; Thomas 1992), and that its age was close to 58 Ma in the Berggren *et al.* (1985) time scale (Eldholm & Thomas 1993). In the time scale of Berggren *et al.* (1995) the extinction is close to 55.5 Ma as proposed by Aubry *et al.* (1996).

The isotope excursions and the benthic faunal extinction were very short events (less than 10^5 years; Kennett & Stott 1991; Robert & Kennett 1994; Aubry *et al.* 1996). We cannot assume that sedimentation rates were constant over the interval between age markers where the event occurred at

Sites 525 and 527, because of the presence of a dissolution interval, suggesting decreased sedimentation rates for a short interval starting just before the extinction. Our measurements of $CaCO_3$ content gave minimum values of 35% at Site 525, 20% at Site 527. At Site 690, where sedimentation rates over the interval between the top of Chron 25 and the nannofossil zone NP9/NP10 boundary were the highest of all sites, $CaCO_3$-values also fluctuate, with minimum values of about 65% just below the benthic extinction (O'Connell 1990; fig. 6 in Thomas 1992).

We used the geomagnetic polarity timescale of Berggren et al. (1995) and the biostratigraphic interpretation of Site 690 of Aubry et al. (1996), giving ages of 55.5 Ma to the benthic extinction event, and 55 Ma to the NP9/NP10 boundary (Berggren & Aubry 1996). We extrapolated age at constant sedimentation rates between 55 and 55.5 Ma, and between 55.5 Ma and the top of Chron 25, using numerical ages as derived from the Berggren et al. (1995) timescale for all age marker levels given in Thomas et al. (1990) for the Maud Rise sites, in Shackleton et al. (1984b) for the Walvis Ridge sites. Then we revised the numerical ages for Site 689 and the Walvis Ridge samples close to the extinction to reflect the supposedly lower sedimentation rates of the intervals with low values of $CaCO_3$. To do this we used the carbon isotope record of Nuttallides truempyi at Site 690 as standard, because sedimentation rates were highest at this site. For the interval between the boundary between NP9 and NP10 and the benthic foraminiferal extinction we revised ages until the carbon isotope curves at Sites 525, 527 and 690 agreed best in general shape (Fig. 3); we then did the same for the Lenticulina spp. isotope record at Site 689. The re-calculation of the ages using the shape of the carbon isotope curve resulted in lower calculated sedimentation rates for the $CaCO_3$-poor sediment interval at the sites. All numerical ages are listed in the appendices.

Fig. 3. Benthic foraminiferal carbon and oxygen isotope excursions at Sites 689, 690, 525 and 527; plotted are uncorrected values for N. truempyi for Sites 690, 525 and 527, for Lenticulina spp. for Site 689, using the geomagnetic polarity timescale of Cande & Kent (1995) and Berggren et al. (1996). Ages of Site 690 after Aubry et al. (1996); ages for the other sites derived by fitting the carbon isotope curves as described in the text.

Sample preparation

Samples for benthic foraminiferal faunal and isotope analysis were dried overnight at 50°C and weighed, then soaked overnight in distilled water. Most samples disaggregated readily and could be washed over a 63 μm screen. For isotope analysis of planktonic foraminifera, samples were split and foraminifera picked from two size fractions: size e (212–250 μm) and size d (300–250 μm) as is standard use in the Cambridge and Oxford isotope laboratories; there were no specimens larger than 300 μm in the Maud Rise samples. We analysed 20–40 specimens of Acarinina mckannai. In a few

samples 'Morozovella' convexa was present in large enough numbers for analysis. Benthic foraminifera for isotope analysis were picked from the > 125 μm size fraction, and we analysed 12–20 specimens. Samples for isotope analysis of the small species Tappanina selmensis consisted of 60–80 specimens. Lenticulina spp. commonly show large fluctuations in isotope values; we excluded from analysis specimens larger than 500 μm, which showed erroneous values, possibly because they resulted from reworking. All specimens were ultrasonicated to remove adhering

microfossils, then dried at 50°C. Foraminifera were transferred to reaction vessels and roasted at 400°C. Bulk samples, weighing a few milligrams, were taken from samples from Cores 525A-32 and 527-24, dried and vacuum roasted at 400°C to remove organic contaminants. The samples were then reacted with 100% orthophosphoric acid at 90°C using a VG Isotech Isocarb common acid bath system. The evolved carbon dioxide was analyzed in a VG isotech SIRA Series II mass spectrometer. The results were calibrated to PDB by repeated analysis of a carbonate standard. Analytical accuracy is better than 0.08‰ for both $\delta^{18}O$ and $\delta^{13}C$.

Benthic foraminifera for faunal analysis were picked from the > 63 μm size fraction, following Thomas (1990a). All specimens counted were picked and mounted in cardboard slides. All samples contained sufficient specimens for analysis (> 250), and counts are shown in the appendices. Taxonomy is as in Thomas (1990a) and largely follows Van Morkhoven et al. (1986). Thomas (1990a) misidentified Neoeponides hillebrandti as Neoeponides lunata and the reverse; that mistake has been rectified in the appendices of this paper. All species richness numbers were recalculated to 100 specimens using rarefaction (Sanders 1968).

Results

Faunas

We define the level of extinction as the interval where species richness declined most rapidly. Pre-extinction faunas at Walvis Ridge and Maud Rise are similar, with almost all species present at all 4 sites (Figs 4, 5, 6, 7), although at varying relative abundances. These faunas contain many cosmopolitan, Late Cretaceous through Paleocene taxa with a large depth range, such as Gavelinella beccariiformis, Gavelinella hyphalus, Neoeponides hillebrandti, Neoeponides lunata, Pullenia coryelli, Bolivinoides delicatulus, Neoflabellina semireticulata and agglutinated taxa such as Tritaxia paleocenica, Tritaxia havanensis and Dorothia oxycona. The agglutinated taxa are more common at Site 527, the deepest site studied. Aragonia velascoensis is rare or absent at Maud Rise, and rare at Site 525 (Fig. 6). Stilostomella spp. are more common at Maud Rise than at Walvis Ridge. Pre-extinction faunas have a very high species richness, with many rare uniserial lagenid species and unilocular taxa. Many common, long-lived species occur, such as Cibicidoides pseudoperlucidus, Oridorsalis umbonatus, Nonion havanense, Nonionella robusta, Anomalina spissiformis and Anomalinoides semicribrata. Overall, bi- and triserial species were less common at Walvis Ridge

than at Maud Rise. Pre-extinction, large peaks in relative abundance of species such as Bulimina thanetensis and S. brevispinosa are not observed at Walvis Ridge. Rectobulimina carpentierae occurs only at the two deeper sites, 527 and 690, with strongly fluctuating relative abundances at the latter site, and Bulimina thanetensis was more common at these sites. Gavelinella beccariiformis was more common at the shallower sites with highest relative abundances at Site 689, in agreement with Katz & Miller (1991) who consider this species typical for bathyal sites at high latitudes. Overall, the pre-extinction faunas were remarkably similar in species composition given the large differences in depth and geographical location, in agreement with Tjalsma & Lohmann (1983) and Kaiho (1988, 1991).

This uniformity ended with the extinction. At Site 690, many of the typical Paleocene species had their last appearance in the highest sample with high diversity, 690B-19H-3, 72–74 cm. In sample 690B-19H-3, 66–68 cm, the diversity decreased from 49 to 26 species per 100 specimens, and bi-triserial species were much more abundant, although in our age model these samples differ in age by only 1000 years. Faunal abundance patterns thus changed at the same level where a high number of last appearances occurred. At Site 689, however, the last appearance of G. beccariiformis and other Paleocene species occurred in sample 689B-23X-1, 80–82 cm, whereas the major drop in species richness from 60 to 42 species per 100 specimens occurred between 23X-1, 80–82 cm and 23X-1, 87–89 cm. Samples 23X-1, 80–82 and 23X-1, 87–89 both contain common T. selmensis and A. aragonensis, typical species for the post-extinction period, but the species richness is high in these samples and G. beccariiformis is present. These appearances might result from bioturbation or core disturbance. At both Maud Rise sites the extinction occurred after a decrease in carbonate content of the sediments to about 65% (O'Connell 1990; Thomas 1992), and after the first appearance of the keeled, warm-water planktonic species 'Morozovella' convexa at high southern latitudes (Stott & Kennett 1990; this paper).

At Walvis Ridge a sharp drop in benthic foraminiferal species richness from 52 to 34 species per 100 specimens occurred between samples 525A-32-6, 145–147 cm and 525A-32-6, 130–132 cm. At Site 527 species richness decreased from 53 to 24 species per 100 specimens between 527-24-2, 56–58 cm and 527-24-2, 38–40 cm. The level of most rapid decrease in species richness is within the lower part of a dark, low-carbonate layer (Table 1): the benthic extinction thus occurred after the onset of increased $CaCO_3$ dissolution. The preservation of benthic foraminifera in this layer of
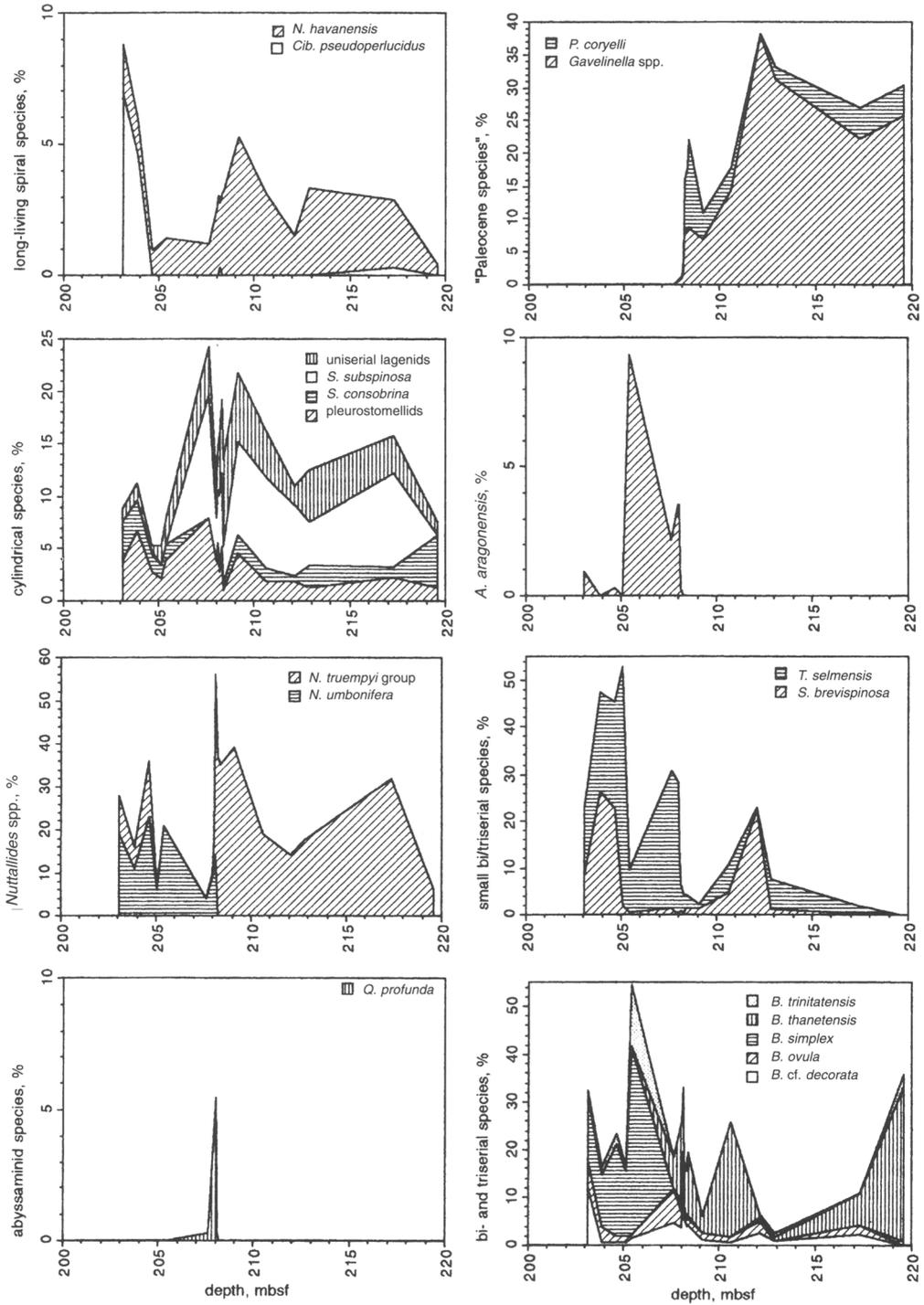
Fig. 4. Benthic foraminiferal relative abundances of most taxa at Site 689; see Appendix 1 for counts.
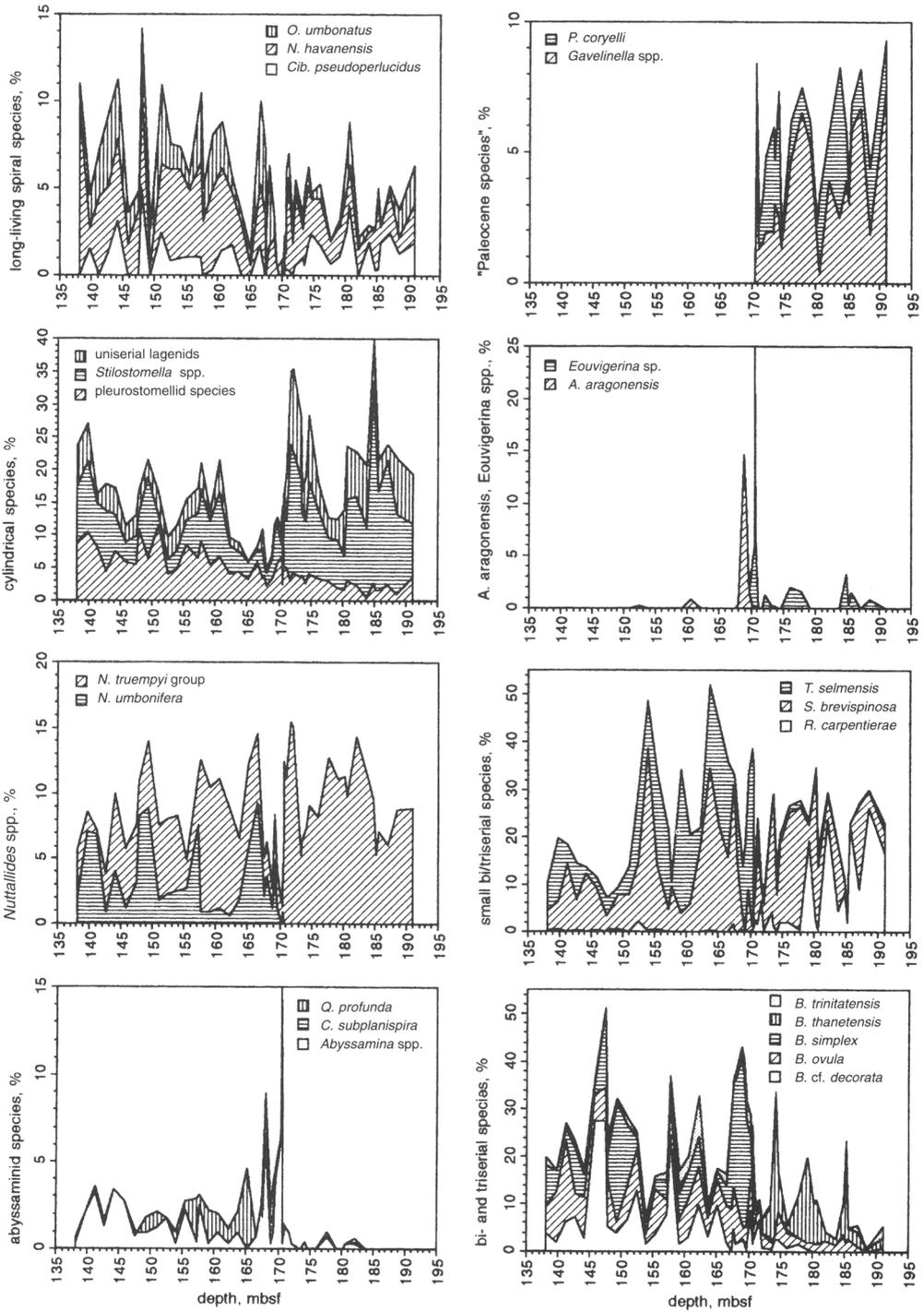
Fig. 5. Benthic foraminiferal relative abundances of the taxa, Site 690; see Appendix for counts.
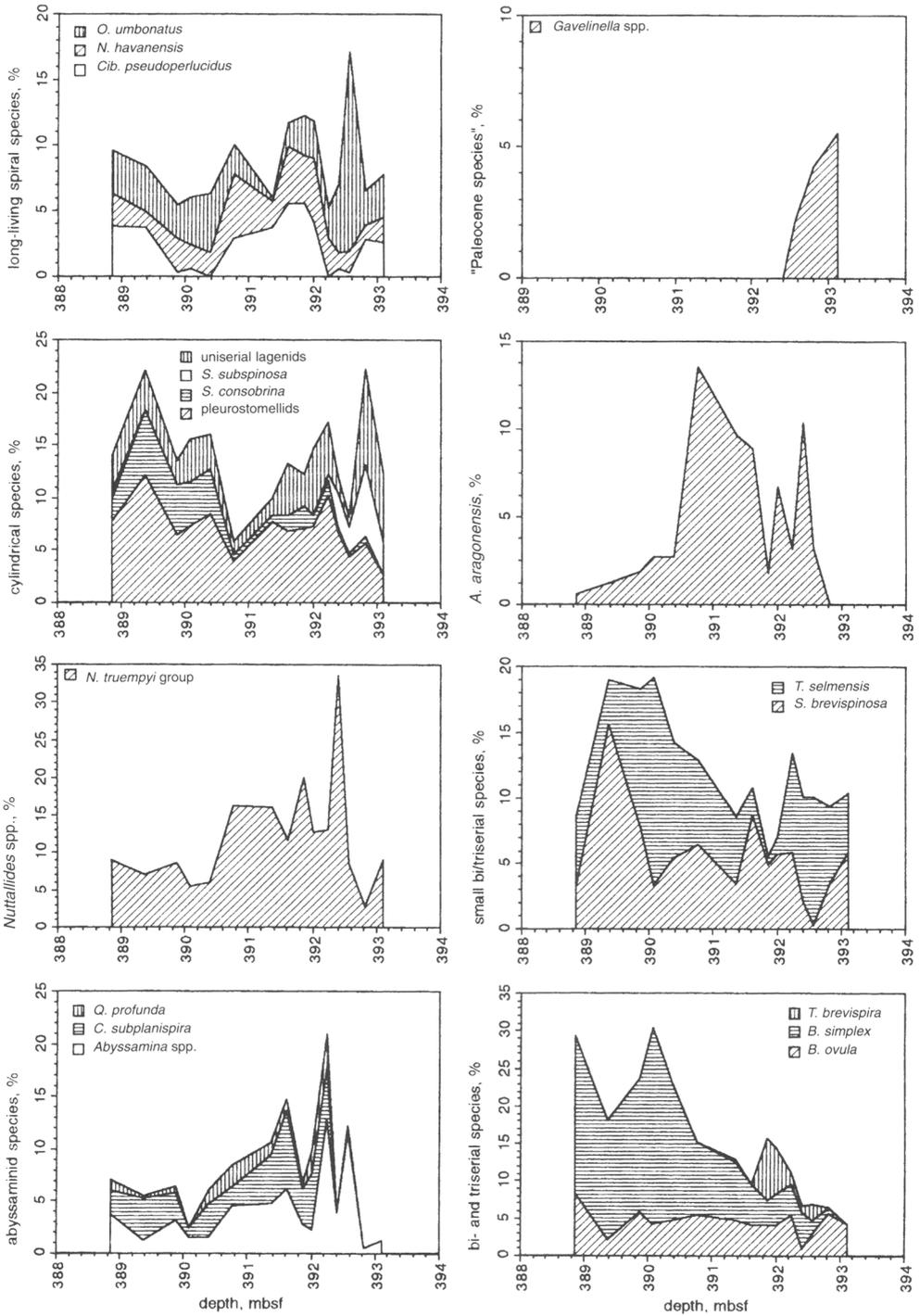
Fig. 6. Benthic foraminiferal relative abundances of the most common taxa at Site 525; see Appendix 2 for counts.
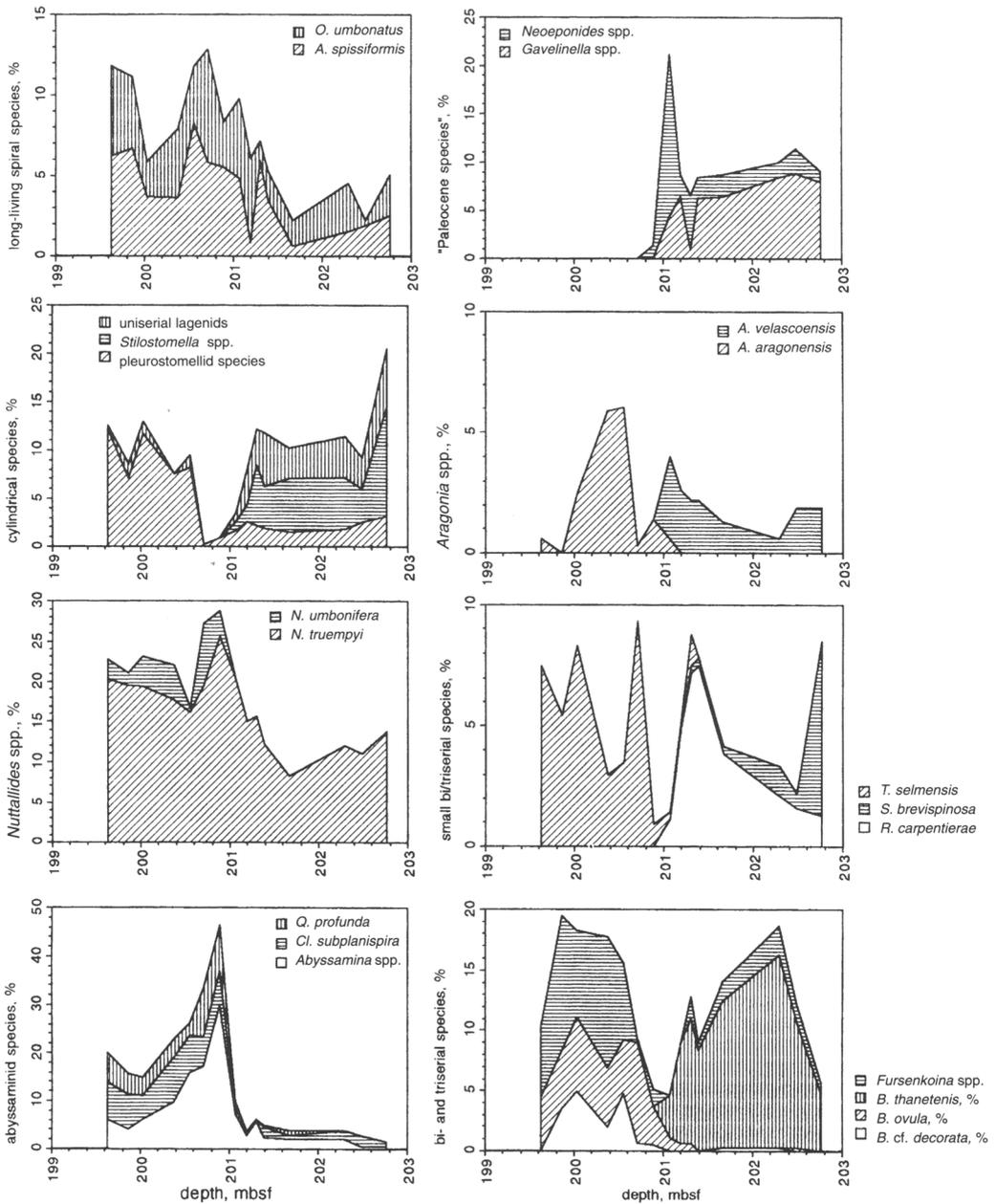
Fig. 7. Benthic foraminiferal relative abundances of the most taxa, Site 527; see Appendix 4 for counts.

low CaCO$_3$-content and increased fragmentation of planktonic foraminifera is good.

The samples in the interval with low diversity in the first 50 000 years after the extinction differ in faunal composition at the sites, with most differences between the Walvis Ridge and the Maud Rise

faunas, lesser differences between the sites at different depths in each area. These faunas occur during the interval with very low δ^{13}C isotopic values at all 4 sites (see below), and thus can be considered coeval. At Site 690, the post-extinction faunas had high relative abundances of *Eouvigerina*

sp., and at both Maud Rise sites *Tappanina selmensis*, *Bolivinoides* cf. *decorata*, *Bulimina ovula*, *Bulimina simplex* and *Bulimina trinitatensis* had high, but strongly fluctuating relative abundances. *N. truempyi* was rare or absent just after the extinction. *Nuttallides umbonifera* first occurred just after the extinction at Maud Rise, but is not present in the samples studied from Walvis Ridge.

At the Maud Rise sites abyssaminid species (small, thin-walled, spiral species; Schnitker 1979; Tjalsma & Lohmann 1983) were more common after the extinction. At Walvis Ridge there was a much stronger increase in the relative abundance of these species, with the highest at the deeper Site 527, in agreement with Tjalsma & Lohmann (1983) and Katz & Miller (1991). In contrast to the patterns at Maud Rise, the post-extinction faunas at Walvis Ridge had very high relative abundances of *Nuttallides truempyi*, as described by Tjalsma & Lohmann (1983) and Katz & Miller (1991) for other Atlantic sites. A distinct drop in relative abundance of biserial and triserial species occurred at Site 527. Slightly higher in the section, however, the biserial species *Tappanina selmensis* and *Aragonia aragonenis* increased in relative abundance, with highest abundances at the shallower site. *Tappanina selmensis* never reached such a high abundance as at the Maud Rise sites (Figs 4, 5, 6, 7). Many rare species (such as lenticulinids, uniserial lagenids, unilocular taxa) were absent at all sites in the post-extinction faunas, at least partially causing the low species richness. Many of these species, however, reappeared higher in the section, and their absence may thus be apparent because of the decreased evenness of the faunas (Signor & Lipps 1982). At counts of about 300 specimens a lower number of species would be observed in an assemblage with higher dominance (Gage & Tyler 1991).

Comparison of the faunas (Fig. 8) showed that at all sites the observed species richness dropped precipitously, with lowest values reached at the deepest Maud Rise site. The species richness appears to recover more quickly at the Walvis Ridge sites, especially at Site 525, if ages are determined according to Fig. 3 (fitting of the $\delta^{13}C$ curve of *N. truempyi*). Interesting is the strong increase in relative abundance of *N. truempyi* at the Walvis Ridge Sites, coeval with its strong decline at both Maud Rise sites. Abyssaminid species increased in relative abundance after the extinction at all sites, but much more so at the Walvis Ridge sites, and the shallower Walvis Ridge site has higher relative abundances of these species than the deeper Maud Rise site. Biserial and triserial species increased in relative abundance just after the extinction at both Maud Rise sites, but decreased

at the deeper Walvis Ridge site and showed little change at Site 525.

A typical component of post-extinction faunas in all oceans are the species *T. selmensis* and *A. aragonensis* (Boersma 1984*b*), although their relative abundances vary from site to site. *T. selmensis* first appeared in the Late Cretaceous, but occurred at low abundances until the extinction event. *A. aragonensis* had its first appearance at the time of the extinction (Tjalsma & Lohmann 1983; Van Morkhoven *et al.* 1986; Bolli *et al.* 1994). *G. beccariiformis* last appeared at all sites at about the same time, although the species started a decline in relative abundance at Site 689 several hundred thousand years earlier (Fig. 4). Overall, however, this pattern does not agree with the statement by Tjalsma & Lohmann (1983) that the *G. beccariiformis* faunas became gradually restricted to shallower depths before becoming extinct. *B. thanetensis* became extinct in the late Paleocene at all sites, but always a few samples higher than *G. beccariiformis*.

Benthic foraminiferal isotopes

We measured stable isotopes in several species of deep sea benthic foraminifera from the Maud Rise sites (Figs 9, 10). We wanted to derive an isotopic record of the extinction event that is as complete as possible, and *N. truempyi* and *Cibicidoides* spp. are not present in large enough numbers for isotope analysis just after the extinction. We also wanted to determine whether species that are presumed to be infaunal or epifaunal because of their morphology (Corliss & Chen 1988; Rosoff & Corliss 1992; Thomas 1990) show a different carbon isotopic signature, as observed in Recent and Neogene taxa (Woodruff & Savin 1985; Zahn *et al.* 1986; Altenbach & Sarnthein 1989; McCorkle *et al.* 1990). Infaunal species precipitate their tests in contact with pore waters, not sea water, and can thus be expected to have lower $\delta^{13}C$ values.

Most species thought to be infaunal because of their morphology had indeed lower $\delta^{13}C$ values than species thought to be epifaunal, with the exception of *Oridorsalis umbonatus*. This long-lived, cosmopolitan, trochospiral species plots in the field of infaunal species (Fig. 10). Its carbon isotope data should thus be interpreted carefully, especially because Rathburn & Corliss (1994) reported that Recent representatives of this taxon live infaunally.

The benthic species show considerable scatter in their isotopic values, and there are differences between the patterns at Sites 689 and 690. At Site 690, *Lenticulina* spp., a presumed infaunal group, shows clear separation in $\delta^{13}C$ values from the epifaunal species, and has consistently lower values
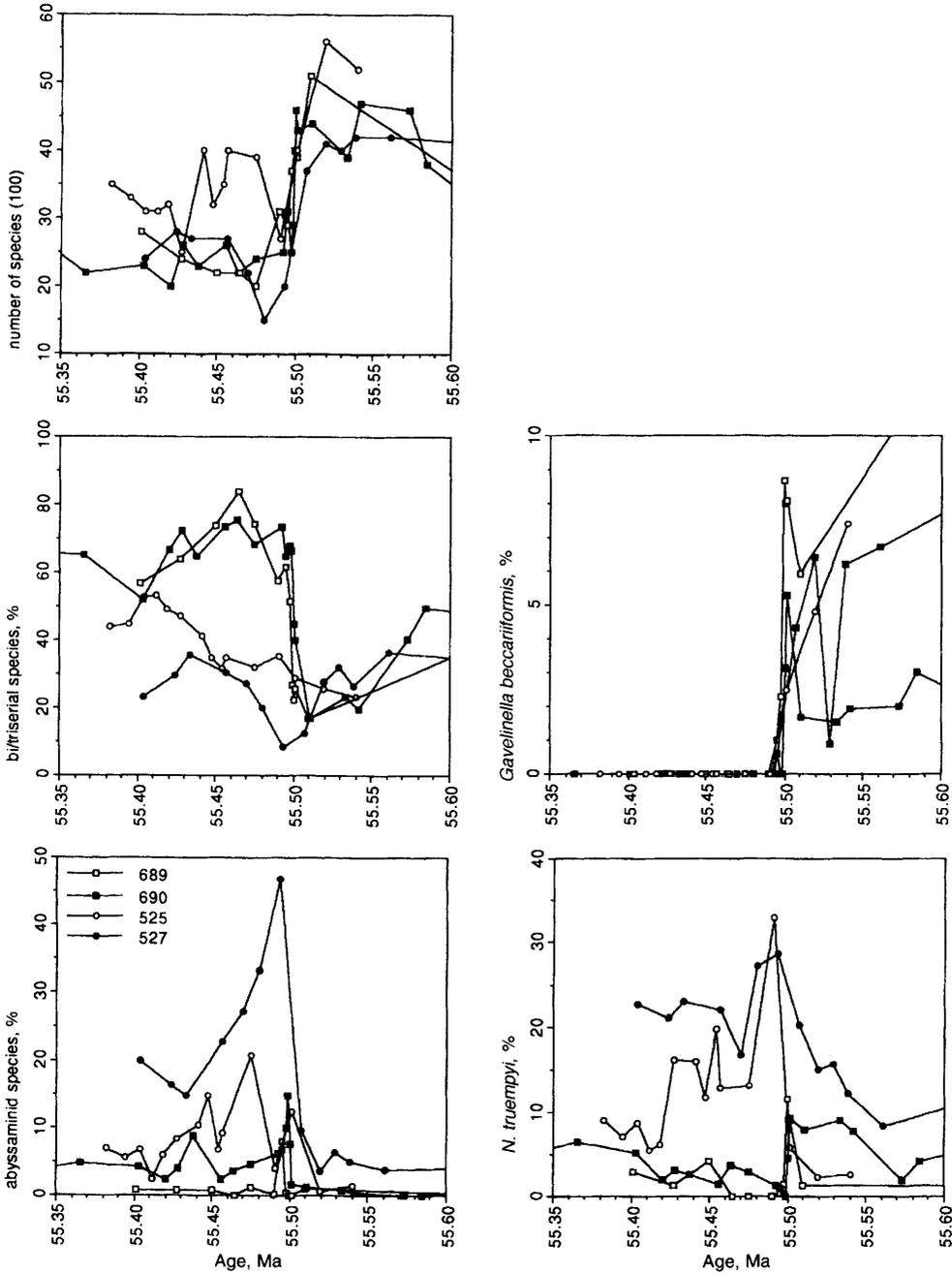
Fig. 8. Number of species (per 100 specimens, calculated by rarefaction, Sanders 1968) and relative abundances of some common species groups of benthic foraminifera, compared for the Walvis Ridge and Maud Rise sites. Closed symbols indicate the deeper site at each location, the open symbols the shallower site.
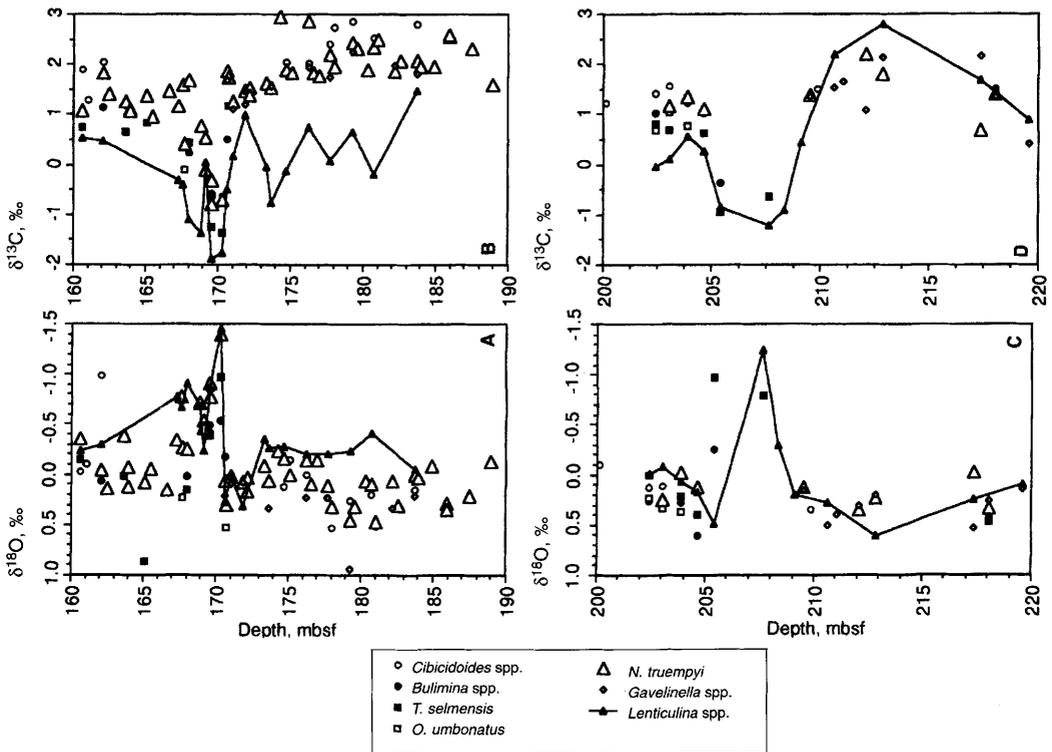
Fig. 9. Oxygen and carbon isotope value for selected benthic foraminiferal species, Sites 689 and 690. Open symbols indicate species considered infaunal because of their morphological resemblance to Recent infaunal taxa (Corliss & Chen 1988; Kaiho 1988, 1991, 1994a; Thomas 1990a); closed symbols show epifaunal species.

than *N. truempyi* (Fig. 9). This is not so at Site 689, and *Lenticulina* spp. values are commonly higher than those of *N. truempyi*. None of the other species in the same samples shows a similar pattern, so that this difference between sites is probably not due to difference in diagenesis. It has been proposed that greater separation in carbon isotopic values of infaunal and epifaunal species results from a higher flux of organic matter to the sea floor (Woodruff & Savin 1985; Zahn *et al.* 1986). With the exception of the interval of anomalously low $\delta^{13}C$ values, the carbon isotopic values of *Lenticulina* spp. are overall lower at Site 690 than at Site 689, thus suggesting a lesser flux of organic matter at the latter site. This is unexpected, because at shallower sites a greater flux of organic matter arrives at the seafloor than at deeper sites at equal productivity (e.g. Berger *et al.* 1994). Higher fluxes of organic matter to the deeper site thus suggest higher productivity at that site. Higher sedimentation rates at Site 690 might be seen as supportive of higher productivity at that site, but

might as well have been caused by admixture of fine terrigenous material (Barker *et al.* 1988).

We can not at present explain why there should have been higher productivity at Site 690, because the sites are very close. Possibly, the pattern of deep-water circulation around Maud Rise caused upwelling at Site 690, on the southwestern flank, but not at Site 689, closer to the top. At present, waters well up along the southwestern flank of the rise (Comiso & Gordon 1982). In the presence of large stratigraphic variations in isotopic values, bioturbation may disturb the signal easily, and we need better age control at Site 689 before we can decide whether the difference in benthic infaunal carbon isotope values at the sites reflects a real environmental difference.

Lenticulina spp. constitute the only group present at both Maud Rise sites over the extinction interval. Comparison of the isotope data of this taxon at both sites (Fig. 9) shows that the excursion had a similar magnitude in the bottom waters of the two sites. Oxygen isotope values at both sites

were not significantly different at both sites before, during or after the excursion.

Isotope excursions

Extreme excursions in carbon and oxygen isotopic values are present in benthic and planktonic foraminiferal records from the Maud Rise sites, and in benthic and bulk records from the Walvis Ridge sites (Figs 3, 11,12,13). Our data for Site 690 agree with those of Kennett & Stott (1990, 1991) and Stott et al. (1996). The benthic foraminiferal extinction was synchronous with a very large, negative, short-term excursion of carbon and oxygen isotopes in planktonic and benthic foraminifera and bulk carbonate (Shackleton & Hall 1990). The isotope excursions reached peak negative values in a few thousand years, and values returned to pre-excursion levels more gradually, in about 50 000 years as estimated at Site 690. We used the isotope excursion to construct the time-scale (see above; Fig. 3), and therefore we assumed that the duration was the same at all 4 sites. The carbon isotope excursion was about $-2\%_o$ for benthic foraminifera at Walvis Ridge and Maud Rise, about $-4\%_o$ for planktonic foraminifera at Maud Rise, leading to decreased vertical gradients.

Bulk carbon isotope values decreased by about $2\%_o$ at the Walvis Ridge sites. The oxygen isotope excursion was about $-1.5\%_o$ for benthic foraminifera at Walvis Ridge (1600–3400 m palaeodepth) and Maud Rise (1100–1900 m palaeodepth), about $-1\%_o$ for planktonic foraminifera at Maud Rise. There are no significant differences in the oxygen isotope values of benthic foraminifera at Sites 689, 690, 525 and 527 over the full interval studied, suggesting little stratification of the water masses at the sites before, during and after the isotope excursions. This observation suggests that intermediate to deep watermasses were poorly stratified, from whatever source they were derived.

Comparison of the planktonic foraminiferal data from Sites 689 and 690 (Fig. 13) shows that oxygen isotopic values were very close throughout the studied sequence, as expected for sites in such close proximity. Possibly the carbon isotope values of planktonic foraminifera were more positive at Site 690, in support of the hypothesis of higher productivity at that site, as outlined above.

Discussion of faunas, isotopes and palaeoenvironments

An investigation of the biogeography of the benthic foraminiferal faunas after the extinction is difficult because many stratigraphical sections have
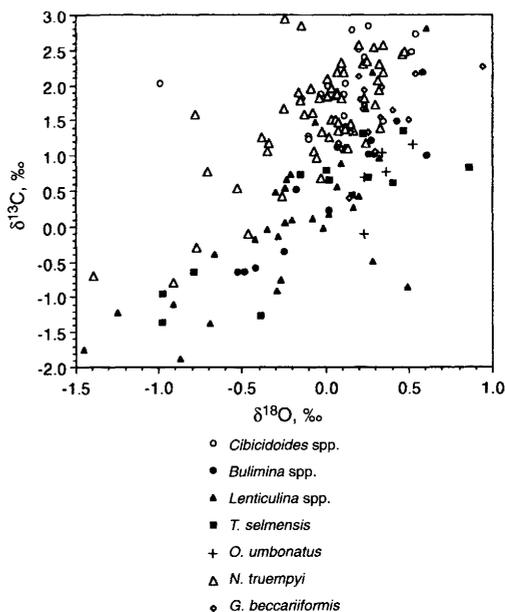
Fig. 10. Scatter plot of $\delta^{13}C$ versus $\delta^{18}O$ values of all benthic foraminiferal data for Sites 689 and 690. Presumed infaunal species (Bulimina spp., T. selmensis, Lenticulina spp.) have closed symbols, presumed epifaunal species (Cibicidoides spp., N. truempyi, Gavelinella spp.) have open symbols. O. umbonatus, which has an epifaunal morphology according to Corliss & Chen (1988) and Kaiho (1988, 1991) is indicated by +, to show its presence within the field of infaunal species.

hiatuses (Aubry et al. 1996). We can therefore only be confident about our time correlations if we compare faunas from the interval of the large, short-lived, negative $\delta^{13}C$-excursion. The benthic foraminiferal extinction shows biogeographical variation between the Walvis Ridge and the Maud Rise sites, which were in the same ocean basin and at similar longitude, separated by about 30° of latitude. The pre-extinction faunas were largely cosmopolitan, with relatively minor differences with location as well as depth (e.g. Kaiho 1988, 1991), but post-extinction faunas show very wide differences in composition. At our sites biogeographical differences were more important than depth differences.

At Maud Rise, the extinction was followed by an increase in relative abundance of species presumed to live infaunally (Corliss & Chen 1988). Such an increase most probably reflects an increase of the flux of particulate organic matter to the sea floor (e.g. Lutze & Coulbourn 1984; Pedersen et al. 1988; Hermelin & Shimmield 1990; Hermelin
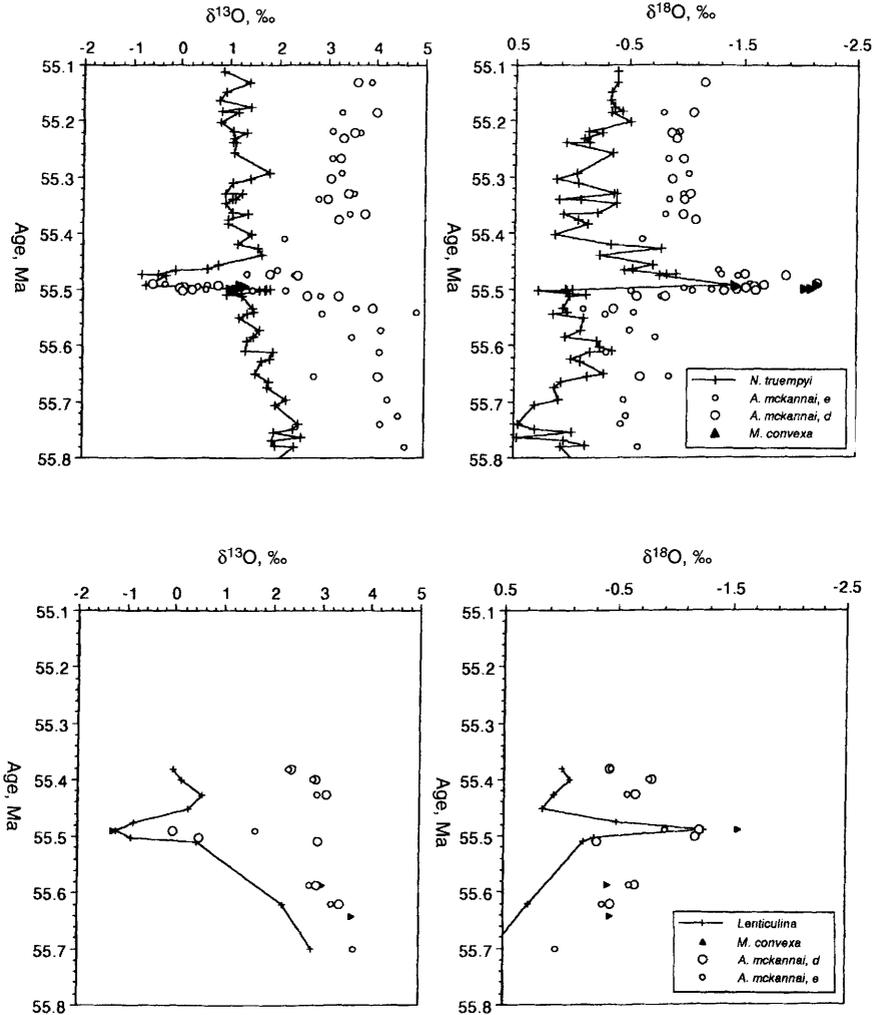
Fig. 11. Carbon and oxygen isotope data for benthic and planktonic foraminifera, Sites 689 and 690. Included are data from Stott *et al.* (1990), Kennett & Stott (1990), and our data.

1992; Rathburn & Corliss 1994), rather than a decrease in dissolved oxygen. This faunal evidence appears to conflict with the carbon isotope data, which show decreased surface-to-deep gradients, suggesting lowered productivity just after the extinction (Kennett & Stott 1991; Fig. 11). We can try to reconcile faunal and isotope data by speculating that the decreased gradients resulted from upwelling of deep, nutrient-rich waters as a result of a changes in deep-water circulation. The upwelling could have caused increased productivity and isotopically lighter total dissolved carbonate in the surface waters. This mechanism can not explain the short-term carbon isotope excursion, and can be only a part of the explanation for the depressed gradients at Sites 689 and 690. We do not suggest that productivity increased worldwide, only that it increased at Maud Rise, and possibly at other sites at high latitudes, or on continental margins, or close to the equator. We suggest that all these sites may have been characterized by increased deposition of organic matter (thus probably increased surface productivity) after the extinction.

In contrast, benthic foraminifera data suggest that the flux of organic matter to the seafloor decreased after the extinction at the Walvis Ridge sites, in line with suggestions that productivity
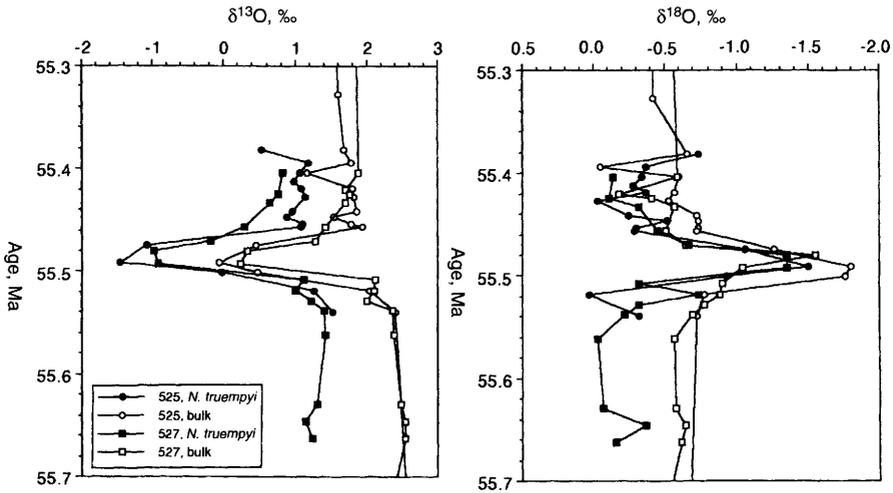
Fig. 12. Carbon and oxygen isotope data for benthic foraminifera and bulk carbonate, Sites 525 and 527. Included are data from Shackleton *et al.* (1984*a*), Shackleton & Hall (1984), and this paper.

decreased globally at the time (e.g. Corfield & Shackleton 1988; Corfield 1993). Thomas (1990) speculated that this difference might have been apparent only, and the result of the fact that many researchers study such a large size fraction (> 125 μm) that the abundant presence of the small, biserial species would go undetected. Data presented in this study, however, clearly show that the difference is real, not the result of difference in size-fraction studied, nor of the presence of hiatuses, since these different faunas coexisted with the short-lived carbon isotope excursion.

Studies from many locations in the Atlantic Ocean have described post-extinction faunas resembling those at the Walvis Ridge sites, with common to abundant abyssaminid species and *N. truempyi* (Clark & Wright 1984; Tjalsma & Lohmann 1984; Katz & Miller 1991; Müller-Merz & Oberhänsli 1991; Oberhänsli *et al.* 1991; Pak & Miller 1992); similar faunas have also been described from land sections in Spain (Zumaya: G. Keller pers. comm. 1994) and Egypt (Speijer 1994). We cannot be certain that these faunas are indeed coeval with the immediate post-extinction faunas because of the lack of isotopic data or low-resolution sampling. At Site 549 in the Bay of Biscay (Reynolds 1992 MSc Thesis, op. cit.) biserial and triserial species increased in relative abundance after the extinction, as at Maud Rise. In the land section at Caravaca (Spain), a similar faunal pattern was observed (G. Keller pers. comm. 1994).

Faunas from some sites in the Indian Ocean show a pattern similar to that at the Atlantic sites,

but we do not know whether we see the immediate post-extinction faunas because of lack of isotope data, poor recovery, or low time resolution. At Site 762 (palaeodepth 1000–1500 m) the post-extinction faunas were dominated by *N. truempyi*, *Cibicidoides* spp., and abyssaminid species; *T. selmensis* and *A. aragonensis* were present (Thomas, unpub. data; R. Nomura pers. comm. 1994). At Site 747 (Kerguelen Plateau, Indian Ocean; palaeodepth 2000–3000 m) post-extinction faunas were dominated by *N. truempyi* , but at the shallower Site 748 (palaeodepth 600–2000 m) *Stilostomella* spp. and *Lenticulina* spp. dominated (Mackensen & Berggren 1992). At Site 752 (palaeodepth 500–1000 m), post-extinction faunas had common *Anomalinoides capitatus/danicus*, *N. truempyi* and *Cibicidoides* spp. (Nomura 1991; R. Nomura pers. comm. 1994). At Site 738 (Indian Ocean, Kerguelen Plateau; Fig. 1) recovery was poor, but the short-term isotope excursion occurred in a recovered interval and is similar in magnitude to that at Maud Rise (Lu & Keller 1993). The benthic foraminiferal extinction occurred in the lower part of an interval of dissolution as at Walvis Ridge, and post-extinction faunas coeval with the carbon isotope negative peak had high relative abundances of *Tappanina selmensis* and small buliminids (Thomas, unpub. data) as at Maud Rise. Later faunas became dominated by *N. truempyi* (R. Nomura pers. comm. 1994).

At equatorial Pacific Site 865 (palaeodepth about 1200 , palaeolatitude 2°N, Bralower *et al.* 1995*a*) post-extinction faunas coeval with the short-lived δ¹³C excursion lack *N. truempyi*, have
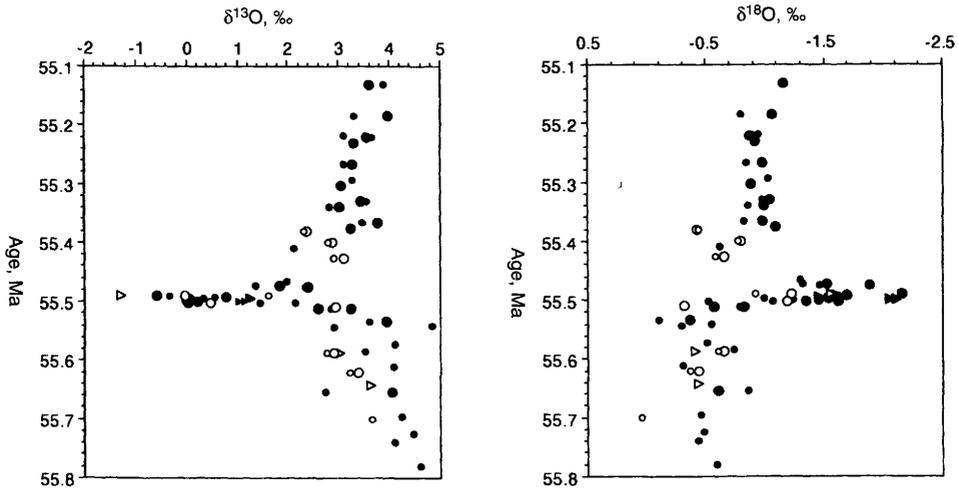
Fig. 13. Carbon and oxygen isotope data for planktonic foraminifera, Sites 689 and 690. Open symbols are data from Site 690, closed symbols are data from Site 689. Circles, *Acarinina mckannai*; triangles, *'Morozovella' convexa*. Included are data from Stott *et al.* (1990), Kennett & Stott (1990), and this paper.

common *Cibicidoides* spp. and *Bulimina semi-costata*, and high relative abundances of bi- and triserial species (Thomas, unpub. data). At Pacific Site 577 (palaeodepth 1500 m) post-extinction faunas show increased relative abundance of *Bulimina semicostata* as well as *N. truempyi* (Miller *et al.* 1987*b*; Pak & Miller 1992), in contrast to the faunal pattern at Site 865, but there may be a hiatus in the immediate post-extinction interval (Corfield & Cartlidge 1992*b*; Berggren *et al.* 1995).

The benthic extinction thus was followed by a period of varying faunas at different locations. At all locations *T. selmensis* and *A. aragonensis* are typical for the post-extinction period at bathyal to abyssal depths. These species might probably be seen as opportunists, quickly filling habitats emptied during the extinction. Species that became extinct included common species thought to have lived epifaunally (e.g. *Neoeponides* spp. and *Gavelinella beccariiformis*), many agglutinant species (e.g. *Dorothia oxycona*, *Tritaxia paleo-cenica*), but also infaunal species such as *B. thanetensis* and *B. delicatulus*. At some locations infaunal morphotypes increased in relative abun-dance for a short period (50 000 years), but at many sites in the Atlantic, Pacific and Indian Oceans epifaunal morphotypes increased in abundance, and infaunal morphotypes were replaced by other infaunal morphotypes (e.g. *Bulimina velascoensis* and *Aragonia velascoensis* before the extinction, *Bulimina semicostata* and *Aragonia aragonensis* after the extinction at Pacific sites; Miller *et al.* 1987*b*; E. Thomas, unpub. data).

It thus appears to be too simplistic to relate the benthic foraminiferal extinction only to increased temperatures with concomitant decreased oxygen levels, although these probably were involved (Thomas 1990; Kaiho 1991). A strong increase in volume of deep to intermediate waters derived from subtropical latitudes rather than from high southern latitudes (as invoked by many authors, including Thomas 1989, 1990, 1992; Kennett & Stott 1990, 1991; Lu & Keller 1993; Zachos et al. 1993) could have caused the observed patterns partially by direct and indirect effects on the deep sea benthic faunas: patterns of aging of intermediate and deep waters, and thus their nutrient and oxygen levels, would change as well as temperature. Probably as important for deep sea faunas, a change in direction of deep water circulation might influence the locations where deep, nutrient-rich waters welled up to the surface, and thus where high surface productivity occurred.

If $\delta^{13}C$ values of deep sea benthic foraminifera during the maximum-excursion were well known from various localities, one might attempt to re-construct the direction of deep water circulation (e.g. Pak & Miller 1992; Zachos *et al.* 1993), lighter values indicating the presence of 'older' deep to intermediate water masses. Lu & Keller (1993) thus argue that the fact that the benthic carbon isotopic excursion was of smaller magni-tude in the Pacific (Pak & Miller 1992) than at Maud Rise (Kennett & Stott 1991) indicates deep-water circulation from Pacific low latitudes to the Antarctic. We do not think that this argument is valid, however, because of the presence of hiatuses

at Site 577 (Corfield & Cartlidge 1992b; Berggren et al. 1996), so that we can not be certain that the observed values reflect the maximum excursion. New isotope data from equatorial Pacific Site 865 suggest that deep waters might have been forming at that location just after the extinction (Bralower et al. 1995b).

It is not clear whether a change in deep-water circulation could be related to decreased levels of dissolved oxygen in shallower marine areas on continental margins (e.g. North Sea Basin: King 1989; Charnock & Jones 1990; New Jersey continental margin: Gibson et al. 1992; southwest Pacific: Moore 1988; Kaiho 1994b; the southern edge of Tethys: Speijer 1994). There might be a link through locally increased productivity (as suggested by Speijer 1994), or decreased levels of dissolved oxygen might have resulted from the high temperatures.

The rapid isotope excursions occurred against the background of longer term events. In the middle Paleocene, bulk carbonate $\delta^{13}C$ values reached a maximum for the Cenozoic (e.g. Shackleton 1986, 1987), which was not higher than more long-term values during the Late Cretaceous (Corfield et al. 1991; Corfield & Cartlidge 1992b). This period of high $\delta^{13}C$ values could be seen as reflecting return to higher oceanic productivity (Shackleton et al. 1985; Shackleton 1986, 1987) after the biosphere recovered from the end-Cretaceous extinction, especially since oceanic $\delta^{13}C$ gradients were very high at the time (Shackleton et al. 1985). This explanation works only if the organic carbon produced was buried in the lithosphere, because $\delta^{13}C$ changes that persist over periods much longer than the residence time of carbon in the ocean can arise only as a result of long-term changes in the global rate of storage of carbon in organic matter rather than in carbonates (Berger & Vincent 1986; Shackleton 1986, 1987; Corfield & Cartlidge 1992b). It is not obvious where the organic matter required to be deposited in the Paleocene was stored, but extensive organic matter-rich deposits of that age occur in southwestern Pacific (Moore 1988), the North Sea region, and possibly oil shales in the continental United States. Carbon isotopic values decreased over a few million years from the middle Paleocene until the early Eocene (Shackleton 1987; Corfield & Cartlidge 1992b). The long-term decreasing values of $\delta^{13}C$ have been tentatively explained by increased erosion of organic carbon rich sediments from the Himalyan orogen (Beck et al. 1995b).

This long-term decrease occurred at a time when oxygen isotope data suggest increasing temperatures of global deep waters as well as surface waters at high latitudes (Shackleton 1986; Corfield & Cartlidge 1992b; Zachos et al. 1994). The high

temperatures have been explained by higher rates of CO_2 emissions from hydrothermal systems (Owen & Rea 1985; Rea et al. 1990) or from plateau basalts (Eldholm & Thomas 1993), especially because preliminary results from studies of chemical proxies for palaeo-CO_2 levels suggest that early Eocene pCO_2 levels were 2 to 6 times present values (Freeman & Hayes 1992; Cerling 1991).

What caused the rapid isotope excursions in the latest Paleocene to be superimposed on these long-term trends? Specifically, did sudden events (e.g. emission of large amounts of volcanic CO_2) trigger the rapid isotope excursions, or did gradual changes cross a threshold-value (Zachos et al. 1994)? Planktonic foraminiferal data from Sites 689 and 690 (Stott et al. 1990, 1996; this paper) and 738 (Lu & Keller 1993) clearly demonstrate that low-latitude, keeled planktonic foraminifera reached high latitudes (> 60°S) before the benthic foraminiferal extinction; extensive warming of high latitude surface waters thus preceded the isotope anomalies. Note that $\delta^{18}O$ values of keeled planktonics at Site 690 are extremely low, while $\delta^{13}C$ values of the same specimens have not reached peak values, suggesting that temperature increase slightly pre-dated the $\delta^{13}C$ excursion (Fig. 11). The rapid oxygen isotope excursion at a time when polar ice-sheets were absent or insignificant should probably be explained by a rapid increase in temperature of high latitude surface waters and deep waters worldwide, by 4–6°C. Such an ocean-wide increase in temperature would have the effect of raising sealevel by about 5–6 m only (Varekamp, pers. comm. 1994), which would not be expected to be noticeable in benthic foraminiferal faunas. Speijer (1994) did not observe a clear sea level signal in neritic sequences in the eastern Mediterranean.

The large, short-term carbon isotope excursion occurred in deep as well as surface waters and in the continental record (Kennett & Stott 1990, 1991; Pak & Miller 1992; Lu & Keller 1993; Stott et al. 1996), and was associated with increased $CaCO_3$-dissolution over a wide depth and geographical range in the deep oceans (Bay of Biscay: Reynolds 1992 MSc Thesis, op. cit.; Stott et al. 1996; Site 738: Lu & Keller 1993; Walvis Ridge: this paper). A large, negative shift in $\delta^{13}C$ composition of total dissolved inorganic carbon as well as increased dissolution and shallowing of the calcium carbonate compensation depth in the oceans could result from a transfer of isotopically light material from the lithosphere or biosphere into the ocean–atmosphere system (Shackleton 1977; Broecker & Peng 1984). The shape of the excursion (rapid start, more gradual return to almost pre-excursion values) is as modelled for disturbance of the ocean–

atmosphere system by transfer of large amounts of isotopically light carbon into the atmosphere (e.g. Kasting & Walker 1993). The rapidity of the initiation of the excursion (a few thousand years) and its short duration suggest that this transfer is not likely to have been caused by changes in ratio of organic carbon to carbonate deposition or erosion (Shackleton 1987; Corfield & Cartlidge 1992b; Walker 1993).

One can estimate how much carbon from the terrestrial biosphere must be transferred to the oceans to explain the short-term carbon shift (Shackleton 1977), if one makes assumptions regarding the size of oceanic and atmospheric reservoirs, and the average isotopic composition of plant material, and if one knew the average, global size of the carbon isotope excursion. Estimates of the average isotopic composition of plant material can be made, assuming that only C3 plants were around in the late Paleocene (Cerling 1993). The amplitude of the carbon isotope excursion is not well constrained, because the event was short and many sections have low sedimentation rates and hiatuses (Aubry et al. 1996); a value between 1 and 2‰, possibly close to 2‰ seems most probable from present observations (Kennett & Stott 1991; Pak & Miller 1992; Stott et al. 1996; Bralower et al. 1995b).

The sizes of atmospheric and oceanic reservoirs are less easy to estimate: the atmospheric reservoir may well have been several times larger than today, which would have led to a larger oceanic reservoir. On the other hand, higher deep ocean temperatures may have caused a decrease in size of the oceanic reservoir. In addition, the size of the oceanic reservoir may have been influenced by the deep sea ventilation rate (Broecker & Takahashi 1984; Thierstein 1989), leading to decreased oceanic reservoir sizes at decreased ventilation rates. Assumption of various values for these parameters, however, indicates that the excursion was so large that transfer of terrestrial biosphere is very unlikely as the cause: such a transfer would require destruction of continental biosphere much larger than that during the end-Cretaceous extinction, which did not occur according to the fossil record.

It is difficult to explain fully such a large shift by rapid emission into the atmosphere of volcanogenic CO_2, derived from the subaerial plateau basalt eruptions of the North Atlantic Volcanic Province (White 1989; White & MacKenzie 1989). The minimum isotopic composition of mid-oceanic ridge volcanic CO_2 is only of the order of −6 to −7‰ (Eldholm & Thomas 1993), so that very large volumes would be necessary. Calculations of the size of plateau-basalt eruptions and the eruption rate required to cause the observed carbon isotope shift have the same problems as the estimates of

biomass required. Average rates of basalt eruption during Chron 24r (several times 10^{13} g CO_2 per year; see Eldholm & Thomas 1993) were certainly too low to cause the excursion. Maximum eruption rates, however, could have been much higher than that (e.g. White & MacKenzie 1989), and an eruption rate of about 100 times the average rate, persisting over a few thousand years, could have been sufficient (Eldholm & Thomas 1993).

The timing of maximum volcanic activity might be seen as problematic for this tentative explanation. The major ash falls, including the most explosive phase of volcanism (ashes −17, +19), clearly postdated the benthic foraminiferal extinction at the Bay of Biscay sites (Knox & Morton 1983, 1988; Backman et al. 1984; Aubry et al. 1986; Knox 1990; Eldholm & Thomas 1993; Berggren & Aubry 1996). We would, however, not necessarily expect high rates of CO_2-effusion resulting from the most explosive volcanic activity, because basaltic (thus less explosive) magmas have the highest concentrations of CO_2 (Gerlach & Taylor 1990). Ashes and basalt flows are present in sediments from nannofossil zone NP9 and the dinoflagellate Apectodinium hyperacanthum zone (Boulter & Manum 1989; Knox 1990; Ali et al. 1992), and Berggren & Aubry (1996) tentatively place the initiation of phase 2 volcanic activity in the lower part of zone NP9. The extinction may be very close in age to the change of volcanic activity from western to eastern Greenland. This change may have triggered the break-up of the continent along the East Greenland margin with ensuing volcanism over very large areas adjacent to the line of break-up, which occurred close the chron C25n/C24r boundary (Larsen et al. 1992).

We can speculate about the following scenario: high latitude surface ocean temperatures increased, possibly as a result of increased atmospheric pCO_2. These high temperatures may have been increased even more by high CO_2 levels from massive plateau basalt eruptions at the initiation of continental break-up, and they caused a decrease in density of surface waters at high latitudes so that a low density lid formed. Therefore formation of deep to intermediate waters at these latitudes decreased in volume, so that waters sinking at subtropical latitudes could increase in volume. The circulation changes caused changes in the location where deep, nutrient-rich waters could well up to the surface, thus influencing productivity of planktonic organisms, and extinction of deep sea benthic foraminifera. The latter extinctions were thus caused by a combination of increased temperature and concomitant decrease in dissolved oxygen concentration, as well as changes in local productivity – either increased or decreased productivity, depending upon location.

In this scenario, dominant deep water formation at subtropical latitudes was probably a short-term phenomenon, lasting not much longer than 50 000 to maybe 100 000 years, because of the self-limiting effect of deep water circulation from lower to higher latitudes (Pak & Miller 1992; Lu & Keller 1993). Such a circulation pattern would increase heat transport to high latitudes, thus further decreasing thermal gradients; but very low gradients would mean decreased speed of atmospheric as well as oceanic currents (as observed in the decreased intensity of dust transport at the time of the benthic extinction; Miller *et al.* 1987; Rea *et al.* 1990; Hovan & Rea 1992). This decreased transport would then cause cooling of high latitudes (Walker & Sloan 1992; Sloan *et al.* 1995), so that deep to intermediate waters could again form there.

There are problems with this simplistic and speculative scenario. We do not think that volcanic CO_2 input can cause the short-term negative $\delta^{13}C$ anomaly by itself. It is not clear whether the total dissolved CO_2 content of the oceans would increase or decrease under this scenario: increased temperatures would lead to a decreased reservoir size, but increased atmospheric pCO_2 would lead to an increased oceanic reservoir (Broecker & Takahashi 1984; Walker 1993). Degassing of the ocean when it was warming up would be expected to lead to increased oceanic $\delta^{13}C$ values, contrary to observations. The increased $CaCO_3$ dissolution suggests increasing dissolved carbonate levels in the oceans (Broecker & Peng 1984; Kasting & Walker 1993). Stott (1992) suggested, on the basis of changes in isotopic composition of organic material in planktonic foraminifera, that atmospheric pCO_2 decreased sharply during the isotope anomalies, possibly as a result of oceanic CO_2 uptake. But data on carbon isotopic composition of organic marine material cannot simply be interpreted as resulting from changes in atmospheric pCO_2, especially for times when other oceanic parameters (temperature, possible alkalinity) were changing (Goericke & Fry 1994; Hinga *et al.* 1994). In addition, we do not know the full effects of the speculative scenario on oceanic productivity and we do not know the average, global effects on productivity changes that vary from place to place.

At the present time, we do not understand the extreme carbon isotope anomalies in the late Paleocene to early Eocene ocean–atmosphere system. More data on the anomalies, including a better understanding of their maximum extent and geographical variability, may lead to a better under-standing of this major disturbance of the global carbon cycle, and thus of the functioning of the carbon cycle itself.

Conclusions

1. The deep sea benthic foraminiferal extinction in the latest Paleocene was coeval with short-term, extreme, negative excursions of $\delta^{13}C$ in planktonic and benthic foraminifera and bulk carbonate, in the South Atlantic and the Weddell Sea, over a range of palaeodepths from 1100–3400 m.

2. The benthic carbon isotope excursion had the same magnitude in both areas, about −2‰. The excursion was a very rapid (beginning in a few thousand years, duration about 50 000 years), and detailed sampling is necessary to evaluate differences in its magnitude in different areas.

3. We do not have enough geographical coverage of the minimum benthic $\delta^{13}C$ values to use these for reconstruction of deep water circulation.

4. Oxygen isotope data indicate rapid warming of high latitude surface waters as well as global deep waters. It is not clear whether this warming was caused by a change in dominant source region of deep to intermediate waters from high to sub-tropical latitudes, or by increased surface water temperatures at high latitudes.

5. The biogeography of benthic foraminiferal assemblages after the extinction suggests that a change in dominant source area of deep water formation was involved.

6. The short-term carbon isotope excursion was so large that it probably could not have been caused by transfer of terrestrial biomass into the ocean–atmosphere system; it was so rapid that it probably could not have been caused by a change in deposition or erosion rates of carbon in carbonate as compared to carbonate in organic matter.

7. We cannot explain the short-term negative carbon isotope excursion, which probably is a complex signal, having global as well as local (productivity) components.

References

ALI, A. E., KING, C. & HAILWOOD, E. A. 1992. Magnetostratigraphic calibration of early Eocene depositional sequences in the southern North Sea Basin. *In*: HAILWOOD, E. A. & KIDD, R. B. (eds) *High Resolution Stratigraphy*. Geological Society, London, Special Publication, **70**, 99–125.

ALTENBACH, A. V. & SARNTHEIN, M. 1989. Productivity record in benthic foraminifera. *In*: BERGER, W. H., SMETACEK, V. S. & WEFER, G. (eds) *Productivity of the Ocean: Present and Past*. Life Science Research Reports, **44**, 255–269.

AUBRY, M.-P. 1992. Paleogene nannofossils from the Kerguelen Plateau, Leg 120. *Proceedings of the Ocean Drilling Program, Scientific Results*, **104**, 471–491.

——, HAILWOOD, E. A. & TOWNSEND, H. A. 1986. Magnetic and calcareous nannofossil stratigraphy of lower Paleogene formations of the Hampshire and London Basins. *Journal of the Geological Society, London*, **143**, 729–735

——, BERGGREN, W. A., KENT, D. V., FLYNN, J. J., KLITGORD, K. D., OBRADOVICH, J. D. & PROTHERO, D. R. 1988. Paleogene chronology: an integrated approach. *Paleoceanography*, **3**, 707–742.

——, ——, STOTT, L. D. & SINHA, A. 1996. The upper Paleocene–lower Eocene stratigraphic record and the Paleocene–Eocene boundary carbon isotope excursion: implications for geochronology. *This volume*.

BACKMAN, J. 1986a.Late Paleocene to middle Eocene calcareous nannofossil biochronology from the Shatsky Rise, Walvis Ridge and Italy. *Palaeogeography, Palaeoclimatology, Palaeoecology*, **57**, 43–59.

—— 1986b. Accumulation patterns of Tertiary calcareous nannofossils around extinctions. *Geologische Rundschau*, **75**, 185–196.

——, MORTON, A. C., ROBERTS, D. G., BROWN, S., KRUMSIECK, K. & MACINTYRE, R. M. 1984. Geochronology of the lower Eocene and upper Paleocene sequences of Leg 81. *Initial Reports of the Deep Sea Drilling Project*, **81**, 877–882.

BARKER, P. F., KENNETT, J. P. ET AL. 1988. *Proceedings of the Ocean Drilling Program, Initial Reports*, **113**.

BARRERA, E. & HUBER, B. 1991. Paleogene and early Neogene oceanography of the southern Indian Ocean: Leg 119 foraminifer stable isotope results. *Proceedings of the Ocean Drilling Program, Scientific Results*, **119**, 693–717.

——, ——, SAVIN, S. M. & WEBB, P. N. 1987. Antarctic marine temperatures: late Campanian through early Paleocene. *Paleoceanography*, **2**, 21–48.

BARRON, E. J. 1987. Eocene equator-to-pole surface ocean temperatures: a significant climate problem? *Paleoceanography*, **2**, 729–740.

—— & PETERSON, W. H. 1991. The Cenozoic ocean circulation based on ocean General Circulation Model results. *Palaeogeography, Palaeoclimatology, Palaeoecology*, **83**, 1–18.

BECK, R. A., BURBANK, D. W., SERCOMBE, W. J., RILEY, G. W., BARNDT, J. K., BERRY, J. R., AFZAL, J., KHAN, A., JURGEN, H., METJE, J., CHEEMA, A., SHAFIQUE, N. A., LAWRENCE, R. D. & KHAN, A. 1995a. Stratigraphic evidence for an early collision between NW India and Asia. *Nature*, **373**, 55–58.

——, ——, ——, OLSON, T. L. & KHAN, A. M. 1995b. Organic carbon exhumation and global warming during the early Himalayan collision. *Geology*, **23**, 387–390.

BECKMANN, J.-P. 1960. Distribution of benthic foraminifera at the Cretaceous-Tertiary boundary of Trinidad (West Indies). *In*: *Report 21st session International Geological Congress, Norden, Copenhagen*. **5**, 57–69.

BERGER, W. H. & VINCENT, E. 1986. Deep-sea carbonates: reading the carbon isotope signal. *Geologische Rundschau*, **75**, 249–269.

——, HERGUERA, J. C., LANGE, C. B. & SCHNEIDER, R. 1994. Paleoproductivity: flux proxies versus nutrient proxies and other problems concerning the Quaternary productivity record. *In*: ZAHN, R., PEDERSEN, T. F., KAMINSKI, M. A. & LABEYRIE, L. (eds) *Carbon Cycling in the Glacial Ocean: Constraints on the Ocean's Role in Global Change*. Springer-Verlag, New York, 385–411.

BERGGREN, W. A. 1992. Paleogene planktonic foraminiferal magnetobiostratigraphy of the southern Kerguelen Plateau (Sites 747–749). *Proceedings of the Ocean Drilling Program, Scientific Results*, **120**, 551–568.

—— & AUBRY, M.-P. 1996. A late Paleocene–early Eocene NW European and North Sea magnetobiostratigraphic correlation network. *This volume*.

—— & MILLER, K. G. 1988. Paleogene planktonic foraminiferal biostratigraphy and magnetobiochronology. *Micropalaeontology*, **34**, 362–380.

—— & —— 1989. Cenozoic bathyal and abyssal calcareous benthic foraminiferal zonation. *Micropaleontology*, **35**, 308–320.

——, KENT, D. V., FLYNN, J. J. & VAN COUVERING, J. A. 1985. Cenozoic geochronology. *Geological Society of America, Bulletin*, **96**, 1407–1418.

——, ——, SWISHER, C. C. III & AUBRY, M.-P 1995. A revised Cenozoic geochronology and chronostratigraphy. *In*: BERGGREN, W. A., KENT, D. V., AUBRY, M.-P & HARDENBOL, J. (eds) *Geochronology, Time Scales and Stratigraphic Correlations: Framework for an Historical Geology*. SEPM Special Publication, **54**.

BOERSMA, A. 1984a. Cretaceous-Tertiary planktonic foraminifera from the south eastern Atlantic, Walvis Ridge area, Deep Sea Drilling Project Leg 74. *Initial Reports of the Deep Sea Drilling Project*, **74**, 501–524.

—— 1984b. Oligocene and other Tertiary benthic foraminifera from a depth traverse down Walvis Ridge, Deep Sea Drilling Project Leg 74. *Initial Reports of the Deep Sea Drilling Project*, **75**, 1273–1300.

—— & PREMOLI-SILVA, I. 1991. Distribution of Paleogene planktonic foraminifera – analogies with the Recent? *Palaeogeography, Palaeoclimatology, Palaeoecology*, **83**, 29–48.

——, —— & SHACKLETON, N. J. 1987. Atlantic Eocene

planktonic foraminiferal paleohydrographic indicators and stable isotope stratigraphy. *Paleoceanography*, **2**, 287–331.

BOLLI, H. M., BECKMANN, J.-P. & SAUNDERS, J. B. 1994. *Benthic Foraminiferal Biostratigraphy of the South Caribbean Region.* Cambridge University Press.

BOLTOVSKOY, E. & BOLTOVSKOY, D. 1988. Cenozoic deep-sea benthic foraminifera: faunal turnovers and paleobiographic differences. *Revue de Micropaléontologie*, **31**, 67–84.

—— & —— 1989. Paleocene–Pleistocene benthic foraminiferal evidence of major paleoceanographic events in the eastern South Atlantic (DSDP Site 525, Walvis Ridge). *Marine Micropaleontology*, **14**, 283–316.

BOULTER, M. C. & MANUM, S. B. 1989. The Brito-Arctic Igneous Province Flora around the Paleocene/Eocene boundary. *Proceedings of the Ocean Drilling Program, Scientific Results*, **104**, 663–680.

BRAGA, G., DEBIASE, R., GRUNIG, A. & PROTO-DECIMA, F. 1975. Foraminiferi bentonici del Paleocene e dell'Eocene della Sezione Posagno. *Schweizerische Paläontologische Abhandlungen*, **97**, 85–111.

BRALOWER, T. J., PARROW, M., THOMAS, E. & ZACHOS, J. C. 1995a. Stable isotope stratigraphy of the Paleogene pelagic cap at Site 865, Allison Guyot. *Proceedings of the Ocean Drilling Program, Scientific Results*, **143**, 581–586.

——, ZACHOS, J. C., THOMAS, E., PARROW, M., PAULL, C. K., KELLY, D. C., PREMOLI-SILVA, I., SLITER, W. V. & LOHMANN, K. C. 1995b. The Paleogene Paleoceanography of the equatorial Pacific Ocean: stable isotopes recorded at ODP Site 865, Allison Guyot. *Paleoceanography*, **10**, 841–865.

BRASS, G. W., SOUTHAM, J. R. & PETERSON, W. H. 1982. Warm saline bottom water in the ancient ocean. *Nature*, **296**, 620–623.

BROECKER, W. S. & PENG, T.-H. 1984. The climate-chemistry connection. *American Geophysical Union Geophysical Monographs*, **29**, 327–336.

—— & TAKAHASHI, T. 1984. Is there a tie between atmospheric CO_2 content and ocean circulation? *American Geophysical Union, Geophysical Monographs*, **29**, 314–326.

BUTLER, R. F., GINGERICH, P. & LINDSAY, E. H. 1981. Magnetic polarity stratigraphy and biostratigraphy of Paleocene and lower Eocene continental deposits, Clark's Fork Basin, Wyoming. *Journal of Geology*, **89**, 299–316.

——, KRAUSE, D. & GINGERICH, P. 1987. Magnetic polarity stratigraphy and biostratigraphy of middle-late Paleocene continental deposits of south–central Montana. *Journal of Geology*, **95**, 647–657.

CANDE, S. C. & KENT, D. V. 1992. A new geomagnetic polarity time scale for the Late Cretaceous and Cenozoic. *Journal of Geophysical Research*, **97** (B10), 13917–13951.

—— & —— 1995. Revised calibration of the geomagnetic polarity time scale for the Late Cretaceous and Cenozoic. *Journal of Geophysical Research*, **100**, 6093–6095.

CHAMBERLIN, T. C. 1906. On a possible reversal of deep-sea circulation and its influence on geologic climates. *Journal of Geology*, **14**, 363–373.

CERLING, T. E. 1991. Carbon dioxide in the atmosphere: evidence from Cenozoic and Mesozoic paleosols. *American Journal of Science*, **291**, 377–400.

CHARNOCK, M. A. & JONES, R. W. 1990. Agglutinated foraminifera from the Palaeogene of the North Sea. *In*: HEMLEBEN, C., KAMINSKI, M. A., KUHNT, W. & SCOTT, D. B. (eds) *Paleoecology, Biostratigraphy, Paleoceanography and Taxonomy of Agglutinated Foraminifera.* Nato Advanced Study Institute Series, Series C, 139–243.

CLARK, M. W. & WRIGHT, R. W. 1984. Paleogene benthic foraminifera from the cape and Angola Basins, South Atlantic Ocean. *Initial Reports of the Deep Sea Drilling Project*, **73**, 459–480.

COLLINSON, M. E. 1983. *Fossil Plants of the London Clay.* Palaeontological Association, London, Field Guides to Fossils, **1**.

COMISO, J. C. & GORDON, J. A. L. 1987. Recurring polynyas over the Cosmonaut Sea and the Maud Rise. *Journal of Geophysical Research*, **92**, 2819–2833.

CORFIELD, R. M. 1993. Depth habitats and the Palaeocene radiation of the planktonic foraminifera monitored using oxygen and carbon isotopes. *In*: LEES, D. & EDWARDS, D. (eds) *Evolutionary Patterns and Processes.* Linnean Society, London, 59–70.

—— & CARTLIDGE, J. E. 1992a. Isotopic evidence for the depth stratification of fossil and recent Globigerinina; a review. *Historical Biology*, **5**, 37–63.

—— & —— 1992b. Oceanographic and climatic implications of the Palaeocene carbon isotope maximum. *Terra Nova*, **4**, 443–445.

—— & SHACKLETON, N. J. 1988. Productivity change as a control on planktonic foraminiferal evolution after the Cretaceous/Tertiary boundary. *Historical Biology*, **1**, 323–343.

——, CARTLIDGE, J. E., PREMOLI-SILVA, I. & HOUSLEY, R. A. 1991. Oxygen and carbon isotope stratigraphy of the Palaeogene and Cretaceous limestones in the Bottaccione Gorge and the Contessa Highway sections, Umbria, Italy. *Terra Nova*, **3**, 414–422.

CORLISS, B. H. & CHEN, C. 1988. Morphotype patterns of Norwegian deep-sea benthic foraminifera and ecological implications. *Geology*, **16**, 716–719.

CROWLEY, T. J. 1991. Past CO_2 changes and tropical sea surface temperatures. *Paleoceanography*, **6**, 387–394.

CUSHMAN, J. A. 1946. *Upper Cretaceous foraminifera of the Gulf Coastal Region of the United States and adjacent areas.* United States Geological Survey Professional Paper, **206**.

ELDHOLM, O. 1990. Paleogene North Atlantic magmatic-tectonic events: environmental implications. *Memorie della Società Geologica Italiana*, **44**, 13–28.

—— & THOMAS, E. 1993. Environmental impact of volcanic margin formation. *Earth and Planetary Science Letters*, **117**, 319–329.

ESTES, R. & HUTCHISON, J. H. 1980. Eocene lower vertebrates from Ellesmere island, Canadian Arctic archipelago. *Palaeogeography, Palaeoclimatology, Palaeoecology*, **30**, 325–347.

FREEMAN, K. H. & HAYES, J. M. 1992. Fractionation of

carbon isotopes by phytoplankton and estimates of ancient CO_2 levels. *Global Biogeochemical Cycles*, **6**, 185–198.

GAGE, J. D. & TYLER, P. A. 1991. *Deep-sea Biology: a Natural History of Organisms at the Deep-sea Floor.* Cambridge University Press.

GERLACH, T. M., & TAYLOR, B. E. 1990. Carbon isotope constraints on the degassing of carbon dioxide from Kilauea Volcano. *Geochimica et Cosmochimica Acta*, **54**, 2051–2058.

GIBSON, T. G., BYBELL, L. M. & OWENS, J. P. 1993. Latest Paleocene lithologic and biotic events in neritic deposits of southwestern New Jersey. *Paleoceanography*, **8**, 495–514.

GINGERICH, P. D. 1983. Paleocene–Eocene faunal zones and a preliminary analysis of Laramide structural deformation of in the Clark's Fork Basin, Wyoming. *Wyoming Geological Association Guidebook*, **34**, 185–195.

GOERICKE, R. & FRY, B. 1994. Variations in marine plankton $\delta^{13}C$ with latitude, temperature and dissolved CO_2 in the world ocean. *Global Biogeochemical Cycles*, **8**, 85–90.

GOLDFARB, R. J., SNEE, L. W., MILLER, L. D. & NEWBERRY, R. J. 1991. Rapid dewatering of the crust deduced from ages of mesothermal gold deposits. *Nature*, **354**, 296–298.

HAQ, B. U., PREMOLI-SILVA, I. & LOHMANN, G. P. 1977. Calcareous plankton biogeographic evidence for major climatic fluctuations in the early Cenozoic Atlantic Ocean. *Journal of Geophysical Research*, **82**, 3861–3876.

HAY, W. W. 1989. Paleoceanography: a review for Geological Society of America Centennial. *Geological Society of America, Bulletin*, **100**, 1934–1956.

HERBERT, T. D. & SARMIENTO, J. L. 1991. Ocean nutrient distribution and oxygenation: limits on the formation of warm saline bottom water over the past 91 m.y. *Geology*, **19**, 702–705.

HERMELIN, J. O. R. 1992. Variations in the benthic foraminiferal fauna of the Arabian Sea: a response to changes in upwelling intensity? *Geological Society of London, Special Publication*, **64**, 151–166

—— & SHIMMIELD, G. B. 1990. The importance of the oxygen minimum zone and sediment geochemistry in the Northwest Indian Ocean. *Marine Geology*, **91**, 1–29.

HINGA, K. R., ARTHUR, M. A., PILSON, M. E. Q. & WHITAKER, D. 1994. Carbon isotope fractionation by marine phytoplankton in culture: the effects of CO_2 concentration, pH, temperature, and species. *Global Biogeochemical Cycles*, **8**, 91–102.

HOOKER, J. J. 1991. The sequence of mammals in the Thanetian and Ypresian of the London and Belgium Basins: location of the Palaeocene–Eocene boundary. *Newsletters on Stratigraphy*, **25**, 75–90.

HORNIBROOK, N. DE B., BRAZIER, R. C. & STRONG, C. P. 1989. Manual of New Zealand Permian to Pleistocene Foraminiferal Biostratigraphy. *New Zealand Geological Survey, Paleontological Bulletin*, **56**.

HOVAN, S. A. & REA, D. K. 1992. Paleocene/Eocene

boundary changes in atmospheric and oceanic circulation: a southern hemisphere record. *Geology*, **20**, 15–18.

JANECEK, T. R. & REA, D. K. 1983. Eolian deposition in the northeast Pacific Ocean: Cenozoic history of atmospheric deposition. *Geological Society of America, Bulletin*, **94**, 730–738.

JENKINS, D. G. & LUTERBACHER, H. 1992. Paleogene Stages and their boundaries (introductory remarks). *Neues Jahrbuch, Geologische und Paläontologische Abhandlungen*, **186**, 1–5.

KAIHO, K. 1988. Uppermost Cretaceous to Paleogene bathyal benthic foraminiferal biostratigraphy of Japan and New Zealand; latest Paleocene–middle Eocene benthic foraminiferal species turnover. *Revue de Paléobiologie, Special Volume*, **2**, 553–559.

—— 1991. Global changes of Paleogene aerobic/anaerobic benthic foraminifera and deep-sea circulation. *Palaeogeography, Palaeoclimatology, Palaeoecology*, **83**, 65–86.

—— 1994a. Benthic foraminiferal dissolved-oxygen index and dissolved oxygen levels in the modern ocean. *Geology*, **22**, 719–722

—— 1994b. Planktonic and benthic foraminiferal extinction events during the last 100 m.y. *Palaeogeography, Palaeoclimatology, Palaeoecology*, **111**, 45–71.

—— & SAITO, S. 1994. Oceanic crust production and climate during the last 100 Myr. *Terra Nova*, **6**, 376–384.

——, MORGANS, H. E. G. & OKADA, H. 1993. Faunal turnover of intermediate-water benthic foraminifera during the Paleogene in new Zealand. *Marine Micropaleontology*, **21**, 51–86.

KASTING, J. F. D. & WALKER, J. C. G. 1993. Long-term effects of fossil-fuel burning and deforestation on levels of atmospheric CO_2. *In*: OREMLAND, R. S. (ed.) *Biogeochemistry of Global Change: Radiatively Active Trace Gases.* Springer-Verlag, New York, 151–165.

KATZ, M. R. & MILLER, K. G. 1991. Early Paleogene benthic foraminiferal assemblage and stable isotope composition in the Southern Ocean, ODP Leg 114. *Proceedings of the Ocean Drilling Program, Scientific Results*, **4**, 481–513.

KEMP, E. M. 1978. Tertiary climatic evolution and vegetation history in the Southeast Indian Ocean region. *Palaeogeography, Palaeoclimatology, Palaeoecology*, **24**, 169–208.

KENNETT, J. P. 1978. The development of planktonic biogeography in the Southern Ocean during the Cenozoic. *Marine Micropaleontology*, **3**, 301–345.

—— & STOTT, L. D. 1990. Proteus and Proto-Oceanus: ancestral Paleogene oceans as revealed from Antarctic stable isotopic results. *Proceedings of the Ocean Drilling Program, Scientific Results*, **113**, 865–880.

—— & —— 1991. Terminal Paleocene deep-sea benthic crisis: sharp deep sea warming and paleoceanographic changes in Antarctica. *Nature*, **353**, 225–229.

KERRICK, D. M. & CALDEIRA, K. 1993. Paleoatmospheric consequences of CO_2 released during early

Cenozoic regional metamorphism in the Tethyan orogen. *Chemical Geology*, **108**, 201–230.

—— & —— 1994. Metamorphic CO_2 degassing and early Cenozoic palaeoclimate. *Geological Society of America Today*, **4**, 57; 62–65.

KING, C. 1989. Cenozoic of the North Sea. *In*: JENKINS D. G. & MURRAY, J. W. (eds) *Atlas of Fossil Foraminifera* (2nd edition). British Micropalaeontological Society Series, Ellis Horwood, London, 418–489.

KLOOTWIJK, C. T., GEE, J. S., PEIRCE, J. W. & SMITH, G. M. 1991. Constraints on the India-Asia convergence: paleomagnetic results from Ninetyeast Ridge. *Proceedings of the Ocean Drilling Program, Scientific Results*, **121**, 777–882.

KNOX, R. W. O'B. 1990. Thanetian and early Ypresian chronostratigraphy in south-east England. *Tertiary Research*, **11**, 57–64.

—— & MORTON, A. C. 1983. Stratigraphical distribution of early Palaeogene pyroclastic deposits in the North Sea Basin. *Proceedings of the Yorkshire Geological Society*, **44**, 355–363.

—— & —— 1988. The record of early Tertiary North Atlantic Volcanism in sediments of the North Sea Basin. *In*: MORTON, A. C. & PARSON, L. M. (eds) *Early Tertiary Volcanism and the Opening of the NE Atlantic*. Geological Society, London, Special Publication, **39**, 407–419.

KOCH, P. L., ZACHOS, J. C. & GINGERICH, P. D. 1992. Coupled isotopic change in marine and continental carbon reservoirs at the Palaeocene/Eocene boundary. *Nature*, **358**, 319–322.

KYTE, F. T., LEINEN, M., ROSS HEATH, G. & ZHOU, L. 1993, Elemental geochemistry of Core LL44-GPC3 and a model for the Cenozoic sedimentation history of the central North Pacific. *Geochimica Cosmochimica Acta*, **57**, 1719–1740.

LARSEN, L. M., PEDERSEN, A. K., PEDERSEN, G. K. & PIASECKI, S. 1992. Timing and duration of Early Tertiary volcanism in the North Atlantic: new evidence from West Greenland. *In*: STOREY, B. C., ALABASTER, T. & PANKHURST, R. J. (eds) *Magmatism and the Causes of Continental Break-up*. Geological Society, London, Special Publication, **68**, 321–333.

LU, G. & KELLER, G. 1993. Climatic and oceanographic events across the Paleocene-Eocene transition in the Antarctic Indian Ocean: inference from planktic foraminifera. *Marine Micropaleontology*, **21**, 101–142.

LUTZE, G. F. & COULBOURN, W. T. 1984. Recent benthic foraminifera from the continental margin of Northwest Africa: community structure and distribution. *Marine Micropaleontology*, **8**, 361–401.

McCORKLE, D. C., KEIGWIN, L.D. JR, CORLISS, B.H. & EMERSON, S. R. 1990. The influence of microhabitats on the carbon isotope composition of deep-sea benthic foraminifera. *Palaeoceanography*, **5**, 161–185.

McGOWRAN, B. 1991. Evolution and Environment in the early Paleogene. *Memoirs of the Geological Society of India*, **20**, 21–53.

McKENNA, M. C. 1980. Eocene paleolatitude, climate, and mammals of Ellesmere Island. *Palaeo-*

geography, Palaeoclimatology, Palaeoecology, **30**, 349–362.

MILLER, K. G., FAIRBANKS, R. G. & MOUNTAIN, G. S. 1987a. Tertiary isotope synthesis, sea level history, and continental margin erosion. *Paleoceanography*, **2**, 1–20,

——, JANECEK, T. R., KATZ, M. R. & KEIL, D. J. 1987b. Abyssal circulation and benthic foraminiferal changes near the Paleocene/Eocene boundary. *Paleoceanography*, **2**, 741–761.

——, KATZ, M. E. & BERGGREN, W. A. 1992. Cenozoic deep-sea benthic foraminifera: a tale of three turnovers. *In*: *BENTHOS '90*, Sendai, Tokai University Press, 67–75.

MACKENSEN, A. & BERGGREN, W. A. 1992. Paleogene benthic foraminifers from the Southern Indian Ocean (Kerguelen Plateau): biostratigraphy and paleoecology. *Proceedings of the Ocean Drilling Program, Scientific Results*, **120**, 603–630.

MANIVIT, H. 1984. Paleogene and Upper Cretaceous calcareous nannofossils from Deep Sea Drilling Project Leg 74. *Initial Reports of the Deep Sea Drilling Project*, **74**, 475–500.

MARKWICK, P.J. 1994. Equability, continentality, and Tertiary climate: the crocodilian perspective. *Geology*, **22**, 613–616.

MATTHEWS, R. K. & POORE, R. Z. 1980. Tertiary ^{18}O record and glacioeustatic sea-level fluctuations. *Geology*, **8**, 501–504.

MOLINA, E., CANUDO, J. I., GUERNET, C., McDOUGALL, K., ORTIZ, N., PASCUAL, J. O., PARES, J. O., SAMSO, J. M., SERRA-KIEL, J. & TOSQUELLA, J. 1992. The stratotypic Ilerdien revisited: integrated stratigraphy across the Paleocene/Eocene boundary. *Revue de Micropaléontologie*, **35**, 143–156.

MOORE, P. R. 1988. Stratigraphy, composition and environment of deposition of the Whangai Formation and associated Late Cretaceous–Paleocene rocks, eastern North Island, New Zealand. *New Zealand Geological Survey, Bulletin*, **100**.

MOORE, T. C. JR, RABINOWITZ, P. D., BORELLA, P. E., SHACKLETON, N. J. & BOERSMA, A. 1984. History of the Walvis Ridge. *Initial Reports of the Deep Sea Drilling Project*, **74**, 873–894.

MÜLLER-MERZ, E. & OBERHÄNSLI, H. 1991. Eocene bathyal and abyssal benthic foraminifera from a South Atlantic transect at 20°–30°S. *Palaeogeography, Palaeoclimatology, Palaeoecology*, **83**, 117–172.

NILSEN, T. H. & KERR, D. R. 1978. Paleoclimatic and paleogeographic implications of a lower Tertiary laterite (latosol) on the Iceland–Faroe Ridge, North Atlantic region. *Geological Magazine*, **115**, 153–236.

NOMURA, R. 1991, Paleoceanography of upper Maestrichtian to Eocene benthic foraminiferal assemblages at ODP Sites 752, 753 and 754, eastern Indian Ocean. *Proceedings of the Ocean Drilling Program, Scientific Results*, **121**, 3–30.

OBERHÄNSLI, H. & HSÜ, K. J. 1986. Paleocene-Eocene Paleoceanography. *In*: *Mesozoic and Cenozoic Oceans*. Geodynamics Series, **15**, 85–100.

——, MÜLLER-MERZ, E. & OBERHÄNSLI, R. 1991. Eocene

Paleoceanographic Evolution at 20°–30°S in the Atlantic Ocean. *Palaeogeography, Palaeoclimatology, Palaeoecology*, **83**, 173–216.

O'CONNELL, S. 1990. Variations in Upper Cretaceous and Cenozoic calcium carbonate percentages, Maud Rise, Weddell Sea, Antarctica. *Proceedings of the Ocean Drilling Program, Scientific Results*, **113**, 971–984.

ODIN, G. S. & LUTERBACHER, H. 1992. The age of the Paleogene Stage Boundaries. *Neues Jahrbuch, Geologische und Paläeontologische Abhandlungen*, **186**, 21–48.

OTTENS, J. J. & NEDERBRAGT, A. J. 1992. Planktic foraminiferal diversity as indicator of ocean environments. *Marine Micropaleontology*, **19**, 13–28.

OLIVAREZ, A. M. & OWEN, R. M. 1989. Plate tectonic reorganizations: implications regarding the formation of hydrothermal ore deposits. *Marine Mining*, **14**, 123–138.

OWEN, R. M. & REA, D. K. 1985. Sea floor hydrothermal activity links climate to tectonics: the Eocene CO_2 greenhouse. *Science*, **227**, 166–169.

PAK, D. K. & MILLER, K. G. 1992. Late Paleocene to early Eocene benthic foraminiferal stable isotopes and assemblages: implications for deepwater circulation. *Palaeoceanography*, **7**, 405–422.

—— & MILLER, K.G. 1995. Isotopic and faunal record of Paleogene deep-water transitions, Leg 145. *Proceedings of the Ocean Drilling Program, Scientific Results*, **145**.

PEDERSEN, T. F., PICKERING, M., VOGEL, J. S., SOUTHON, J. N. & NELSON, D. E. 1988. The response of benthic foraminifera to productivity cycles in the eastern equatorial Pacific: faunal and geochemical constraints on glacial bottom water oxygen levels. *Palaeoceanography*, **3**, 157–168.

POSPICHAL, J.J. & WISE, S.W. JR. 1990. Paleocene to middle Eocene calcareous nannofossils of ODP Sites 689 and 690, Maud Rise, Weddell Sea. *Proceedings of the Ocean Drilling Program, Scientific Results*, **113**, 613–638.

PREMOLI-SILVA, I. & BOERSMA, A. 1984. Atlantic Eocene planktonic foraminiferal historical biogeographic and paleohydrologic indices. *Palaeogeography, Palaeoclimatology, Palaeoecology*, **67**, 315–356.

PRENTICE, M. L. & MATTHEWS, R. K. 1988. Cenozoic ice-volume history: development of a composite oxygen isotope record. *Geology*, **16**, 963–966.

RATHBURN, A. E. & CORLISS, B. H. 1994. The ecology of living (stained) deep-sea benthic foraminifera from the Sulu Sea. *Palaeoceanography*, **9**, 87–150.

RAUP, D. M. & SEPKOSKI, J. J. 1986. Periodic extinction of families and genera. *Science*, **231**, 833–836.

REA, D. K. 1994. The paleoclimate record provided by Eolian deposition in the deep sea: the geologic history of wind. *Reviews in Geophysics*, **32**, 159–195.

——, ZACHOS, J. C., OWEN, R. M. & GINGERICH, D. 1990. Global change at the Paleocene-Eocene boundary: climatic and evolutionary consequences of tectonic events. *Palaeogeography, Palaeoclimatology, Palaeoecology*, **79**, 117–128.

ROBERT, C. & CHAMLEY, H. 1991. Development of early Eocene warm climates, as inferred from clay mineral variations in oceanic sediments. *Palaeogeography, Palaeoclimatology, Palaeoecology (Global and Planetary Change)*, **89**, 315–332.

—— & KENNETT, J. P. 1992. Paleocene and Eocene kaolinite distribution in the South Atlantic and Southern Ocean: Antarctic climatic and paleoceanographic implications. *Marine Geology*, **103**, 9–110.

—— & —— 1994. Antarctic subtropical humid episode at the Paleocene–Eocene boundary: clay mineral evidence. *Geology*, **22**, 211–214.

—— & MAILLOT, H. 1990. Paleoenvironments in the Weddell Sea area and Antarctic climates as deduced from clay mineral associations and geochemical data, ODP Leg 113. *Proceedings of the Ocean Drilling Program, Scientific Results*, **113**, 51–70.

ROBERTS, D. G., MORTON, A. C. & BACKMAN, J. 1984. Late Paleocene–Eocene volcanic events in the northern North Atlantic Ocean. *Initial Reports of the Deep Sea Drilling Project*, **81**, 913–923.

ROMEIN, A. J. T. 1979. Lineages in early Paleogene calcareous nannoplankton. *Utrecht Micropaleontology Bulletin*, **22**.

ROSOFF, D. B. & CORLISS, B. H. 1992. An analysis of Recent deep-sea benthic foraminiferal morphotypes from the Norwegian and Greenland Seas. *Palaeogeography, Palaeoclimatology, Palaeoecology*, **91**, 13–20.

SANDERS, H. L. 1968. Marine benthic diversity: a comparative study. *American Naturalist*, **102**, 243–282.

SCHMIDT, K.-H. 1991. Tertiary palaeoclimatic history of the southeastern Colorado Plateau. *Palaeogeography, Palaeoclimatology, Palaeoecology*, **86**, 283–296.

SCHNITKER, D. 1979. Cenozoic deep water benthic foraminifers, Bay of Biscay. *Initial Reports of the Deep Sea Drilling Project*, **48**, 377–414.

SCHROEDER, T. 1992. A palynological zonation for the Paleocene of the North Sea Basin. *Journal of Micropalaeontology*, **11**, 113–125.

SELVERSTONE, J. & GUTZLER, D. S. 1993. Post-125 Ma carbon storage associated with continent-continent collision. *Geology*, **21**, 885–888.

SETO, K., NOMURA, R. & NIITSUMA, N. 1991. Data report: oxygen and carbon isotope records of the upper Maestrichtian to lower Eocene benthic foraminifers at Site 752 in the Eastern Indian Ocean. *Proceedings of the Ocean Drilling Program, Scientific Results*, **121**, 885–889.

SHACKLETON, N. J. 1977. Carbon-13 in *Uvigerina*: tropical rainforest history and the equatorial Pacific carbonate dissolution cycles. *In*: ANDERSEN, N. R. & MALAHOFF, A. (eds) *The Fate of Fossil Fuel CO_2 in the Oceans*. Plenum Press, New York, 401–447.

—— 1986. Paleogene stable isotope events. *Palaeogeography, Palaeoclimatology Palaeoecology*, **57**, 91–102.

—— 1987. The carbon isotope history of the Cenozoic. *In*: BROOKS, J. & FLEET, A. J. (eds) *Petroleum Source Rocks*. Blackwell, 427–438.

—— & BOERSMA, A. 1981. The climate of the Eocene ocean. *Journal of the Geological Society of London*, **138**, 153–157.

—— & HALL, M. A. 1984. Carbon isotope data from Leg 74 sediments. *Initial Reports of the Deep Sea Drilling Project*, **74**, 613–619.

—— & —— 1990. Carbon isotope stratigraphy of bulk sediments, ODP Sites 689 and 690, Maud Rise, Antarctica. *Proceedings of the Ocean Drilling Program, Scientific Results*, **113**, 985–989.

——, CORFIELD, R. M. & HALL, M. A. 1985. Stable isotope data and the ontogeny of Palaeocene planktonic foraminifera. *Journal of Foraminiferal Research*, **15**, 321–336.

——, HALL, M. A. & BLEIL, U. 1985. Carbon isotope stratigraphy, Site 577. *Initial Reports of the Deep Sea Drilling Project*, **86**, 503–511.

——, —— & BOERSMA, A. 1984*a*. Oxygen and carbon isotope data from Leg 74 foraminifers. *Initial Reports of the Deep Sea Drilling Project*, **74**, 599–612.

—— & members of the Scientific Party. 1984*b*. Accumulation rates in Leg 74 sediments. *Initial Reports of the Deep Sea Drilling Project*, **74**, 621–637.

SIGNOR, P. & LIPPS, J. 1982. Sampling bias, gradual extinction patterns, and catastrophes in the fossil record. *In*: Geological Society of America, Special Publication, **193**, 291–296.

SLOAN, L. & BARRON, E. J. 1992. A comparison of Eocene climate model results to quantified paleoclimatic interpretations. *Palaeogeography, Palaeoclimatology, Palaeoecology*, **93**, 183–202.

——, ——, REA, D. K. & ZACHOS, J. C. 1992. Possible methane-induced polar warming in the early Eocene. *Nature*, **357**, 320–322.

——, WALKER, J. C. G. & MOORE T. C. JR. 1995. The possible role of oceanic heat transport in early Eocene climate. *Paleoceanography*, **10**, 347–356.

SMITH, H. A., CHAMBERLAIN, C. P. & ZEITLER, P. K. 1994. Timing and duration of Himalyan metamorphism within the Indian Plate, Northwest Himalaya, Pakistan. *Journal of Geology*, **102**, 493–508.

SPEIJER, R. P. 1994, Extinction and recovery patterns in benthic foraminiferal paleocommunities across the Cretaceous/Paleogene and Paleocene/Eocene boundaries. *Geologica Ultraiectina*, **124**.

SPIEß, V. 1990. Cenozoic magnetostratigraphy of Leg 113 drill sites, Maud Rise, Weddell Sea, Antarctica. *Proceedings of the Ocean Drilling Program, Scientific Results*, **113**, 261–315.

STAUDIGEL, H., HART, S. R., SCHMINCKE, H.-U. & SMITH, B. M. 1989. Cretaceous ocean crust at ODP Sites 417 and 418: carbon uptake from weathering versus loss by magmatic outgassing. *Geochimica et Cosmochimica Acta*, **53**, 3091–3094.

STOTT, L. D. 1992. Higher temperatures and lower oceanic pCO₂: a climate enigma at the end of the Paleocene epoch. *Paleoceanography*, **7**, 395–404.

—— & Kennett, J. P. 1990. Antarctic Paleogene planktonic foraminiferal biostratigraphy: ODP Leg 113, Sites 689 and 690. *Proceedings of the Ocean Drilling Program, Scientific Results*, **113**, 549–570

——, ——, SHACKLETON, N. J. & CORFIELD, R. M. 1990. The evolution of Antarctic surface waters during the Paleogene: inferences from the stable isotopic

composition of planktonic foraminifera, ODP Leg 113. *Proceedings of the Ocean Drilling Program, Scientific Results*, **113**, 849–864.

——, SINHA, A., THIRY, M., AUBRY, M.-P. & BERGGREN, W. A. 1996. Global $\delta^{13}C$ changes across the Paleocene/Eocene boundary: criteria for terrestrial–marine correlations. *This volume*.

THIERSTEIN, H. R. 1989. Inventory of Paleoproductivity Records: the Mid-Cretaceous enigma. *In*: BERGER, W. H., SMETACEK V. S. & WEFER, G. (eds) *Productivity of the Ocean: Present and Past*. Life Science Reports, **44**, 355–375.

THOMAS, E. 1989. Development of Cenozoic deep-sea benthic foraminiferal faunas in Antarctic waters. *In*: CRAME, J. A. (ed.) *Origins and Evolution of Antarctic Biota*. Geological Society of London, Special Publication, **47**, 283–296.

—— 1990*a*. Late Cretaceous through Neogene deep-sea benthic foraminifers, Maud Rise, Weddell Sea, Antarctica. *Proceedings of the Ocean Drilling Program, Scientific Results*, **113**, 571–594.

—— 1990*b*. Late Cretaceous–early Eocene mass extinctions in the deep sea. *In*: Sharpton, V. L. & Ward, P. D. (eds) *Global Catastrophes in Earth History* Geological Society of America, Special Publication, **247**, 481–495.

—— 1992. Cenozoic deep-sea circulation: evidence from deep-sea benthic foraminifera. *American Geophysical Union, Antarctic Research Series*, **56**, 141–165.

——, BARRERA, E., HAMILTON, N., HUBER, B. T., KENNETT, J. P., O'CONNELL, S., SPIEß, V., WEI, W. & WISE, S. W. JR 1990. Upper Cretaceous–Paleogene stratigraphy of Sites 689 and 690, Maud Rise (Antarctica). *Proceedings of the Ocean Drilling Program, Scientific Results*, **113**, 901–914.

——, SHACKLETON, N. J. & HALL, M. A. 1992. Carbon isotope stratigraphy of Paleogene bulk sediments, Hole 762C (Exmouth Plateau, eastern Indian Ocean). *Proceedings of the Ocean Drilling Program, Scientific Results*, **122**, 897–901.

TJALSMA, R. C. & LOHMANN, G. P. 1983. *Paleocene–Eocene bathyal and abyssal benthic foraminifera from the Atlantic Ocean*. Micropaleontology Special Publication, **4**.

TONARINI, S., VILLA, A. M., OBERLI, F., MEIER, M., SPENCER, D. A., POGNANTE, U. & RAMSAY, D. A. 1993. Eocene age of eclogite metamorphism in Pakistan Himalaya: implications for India–Eurasia collision. *Terra Nova*, **5**, 13–20.

TOURET, J. L. R. 1992. CO₂ transfer between the upper mantle and the atmosphere: temporary storage in the lower continental crust. *Terra Nova*, **4**, 87–98.

VAN MORKHOVEN, F. P. C., BERGGREN, W. A. & EDWARDS, A. S. 1986. *Cenozoic cosmopolitan deep-water benthic foraminifera*. Elf-Aquitaine, Pau, France.

VON HILLEBRANDT, A. 1962. Das Paläozäne und seine Foraminiferenfauna im Becken von Reichenhall und Salzburg. *Bayerische Akademie der Wissenschaften, Mathematisch–Naturwissenschaftliche Klasse, Abhandlungen, Neue Folge*, **108**.

VAREKAMP, J. C., KREULEN, R., POORTER, R. P. E. & VAN BERGEN, M. J. 1992. Carbon sources in arc volcanism, with implications for the carbon cycle.

Terra Nova, **4**, 363–373.

WALKER, J. C. G. 1993. Biogeochemical Cycles of carbon on a Hierarchy of Time Scales. *In*: OREMLAND, R. S. (ed.) *Biogeochemistry of Global Change: Radiatively Active Trace Gases*. Springer-Verlag, New York 3–28.

—— & SLOAN, L. 1992. Something is wrong with climate theory. *Geotimes*, **June**, 16–18.

WHITE, R. S. 1989. Igneous outbursts and mass extinctions. *EOS, Transactions American Geophysical Union*, **70**, 1480, 1490–1491.

—— & MACKENZIE, D. 1989. Magmatism at riftzones: the generation of volcanic continental margins and flood basalts. *Journal of Geophysical Research*, **94**, 7685–7729.

WILLIAMS, C. A. 1986. An oceanwide view of Palaeogene plate tectonics. *Palaeogeography, Palaeoclimatology, Palaeoecology*, **57**, 3–25.

WING, S. L. 1984. A new basis for recognizing the Paleocene/Eocene boundary in western interior North America. *Science*, **226**, 439–441.

——, BOWN, T. M. & OBRADOVICH, J. D. 1991. Early Eocene biotic and climatic change in interior western America. *Geology*, **19**, 1189–1192.

WOLFE, J. A. 1978. A paleobotanical interpretation of Tertiary climates in the northern hemisphere. *American Scientist*, **66**, 694–703.

—— & POORE, R. Z. 1982. Tertiary marine and non-marine climatic trends. *In*: *Climate in Earth History*. National Academy Press, for the American Geophysical Union, 154–148.

WOODRUFF, F. & SAVIN, S. M. 1985. $\delta^{13}C$ values of Miocene Pacific benthic foraminifera: correlations with sea level and biological productivity. *Geology*, **13**, 119–122.

ZACHOS, J., REA, D., SETO, K., NOMURA, R. & NIITSUMA, N. 1992. Paleogene and early Neogene deep water paleoceanography of the Indian Ocean as determined from benthic foraminifer stable carbon and oxygen isotope records. *American Geophysical Union, Geophysical Monographs*, **70**, 351–386.

——, LOHMANN, K. C., WALKER, J. C. G. & WISE, S. W. 1993. Abrupt climate change and transient climates during the Paleogene: a marine perspective. *Journal of Geology*, **101**, 191–213.

——, STOTT, L. D. & LOHMANN, K. C. 1994. Evolution of early Cenozoic temperatures. *Paleoceanography*, **9**, 353–387.

ZAHN, R., WINN, K. & SARNTHEIN, M. 1986. Benthic foraminiferal $\delta^{13}C$ and accumulation of organic carbon: *Uvigerina peregrina* group and *Cibicidoides wuellerstorfi*. *Paleoceanography*, **1**, 27–42.

Appendix 1. *Faunal data, Site 689*

sample	depth, mbsf	age, Ma	number of species	number of species (100)	number of specimens	Abyssamina poagi	Abyssamina quadrata	Alabamina creta	Allomorphina trigona	Anomalinoides acutus	Anomalinoides capitatus	Anomalinoides semicribratus	Anomalinoides spissiformis	Anomalinoides spp.	Aragonia aragonensis	Aragonia velascoensis	Bolivinoides cf. decorata	Bolivinoides delicatulus	Bolivinoides laevigatus	Bulimina macilenta	Bulimina midwayensis	Bulimina ovula	Bulimina cf. semicostata	Bulimina simplex	Bulimina thanetensis	Bulimina trinitatensis	Buliminella beaumonti	Ceratobulimina sp. small	Cibicidoides dayi
22H-4, 108-116	203.08	55.401	42	28	319	2								3	3		38				18			43	5				
22H-5, 40-42	203.91	55.427	32	24	373										5		2				12			41	6				
22H-5,113-118	204.63	55.450	28	22	318	2								3	1		2				4			61	7				
22H-6, 8-12	205.10	55.465	33	22	323									3			2				4			44	2	1				1
22H,CC	205.43	55.475	27	20	353	4								2	33		5				2			139	1	45			
23X-1, 40-42	207.61	55.490	43	31	326										7		15				23			22					
23X-1, 80-82	208.01	55.495	42	29	313									11	11		11		1		11	7		52					
23X-1, 87-89	208.08	55.498	60	37	394			1	1				4	2	14		50		2		26	1		43	10	1			14
23X-1, 94-96	208.15	55.499	66	40	357				1				11	5	1		21	2	1		9			32		2			
23X-1,106-108	208.27	55.500	53	40	287								10	2			11		2		4			30		2	2		
23X-1,116-119	208.38	55.501	56	39	310								16				13				4		2	41			2		
23X-2, 40-42	209.11	55.510	68	51	304			1	1				7	1		1	3		8		1		5	11		1		2	
23X-3, 42-44	210.61	55.621	52	34	319								2				2				1	3		77					
23X-4, 40-42	212.11	55.700	46	29	327								5				8		3		8	3		2		1			
23X,CC	212.85	55.980	43	34	239								18	2			2							2		2	3		
24X-1, 42-44	217.33	56.242	56	38	310								8				7		3				6	21			6	2	
24X,CC	219.56	56.373	33	24	237								1				3					2		77	6				

sample	depth, mbsf	age, Ma	number of species	number of species (100)	number of specimens	Lenticulina spp.	Neoflabellina reticulata	Neoeponides hillebrandti	Neoeponides lunata	Nonion havanense	Nonionella longicamerata	Nonionella robusta	Nuttallides umbonifera	Nuttallides truempyi	Nuttallides sp. flat	Nuttallides sp. high	Nuttallinella florealis	Oridorsalis nitidus	Oridorsalis umbonatus	Orthomorphina spp.	Osangularia navarroana	Osangularia velascoensis	polymorphinid species	pleurostomellid species	Patellina corrugata	Pseudoparrella sp.	Pseudopatellinelloides sp.	Pullenia bulloides	Pullenia coryelli	Pullenia jarvisi
22H-4, 108-116	203.08	55.401	42	28	319	6				6	1	1	19	9					15				1	12						
22H-5, 40-42	203.91	55.427	32	24	373	10				5		4	11	5					19	5			1	25						
22H-5,113-118	204.63	55.450	28	22	318	8				3	2	1	23	13					4					9						
22H-6, 8-12	205.10	55.465	33	22	323	8				4		4	6						1					7						
22H,CC	205.43	55.475	27	20	353	21				5		2	21						4	4				14						
23X-1, 40-42	207.61	55.490	43	31	326	9				4		1	4						3	9				26						
23X-1, 80-82	208.01	55.495	42	29	313	3			1	8			9	1					13	5		1	5	12					1	
23X-1, 87-89	208.08	55.498	60	37	394	12			1	8			12	1	12	6			3				4	22	2			5		
23X-1, 94-96	208.15	55.499	66	40	357	12			1	5	9			14	41	1			2				3	10				27		
23X-1,106-108	208.27	55.500	53	40	287	17	2	2		9			26	11		2			1					12				28		3
23X-1,116-119	208.38	55.501	56	39	310	18			1	5	10		28	7	1				6	3	1			3				41		4
23X-2, 40-42	209.11	55.510	68	51	304	31				16	2	2	4	35	5			1	5				2	14				12		3
23X-3, 42-44	210.61	55.621	52	34	319	16				10		2	4	14	1			5	3				4	6				11		3
23X-4, 40-42	212.11	55.700	46	29	327	7	1			5	1	2	10	4					2	3			3	6	1				1	
23X,CC	212.85	55.980	43	34	239	21				8			18						2	1			3	3				4		
24X-1, 42-44	217.33	56.242	56	38	310	18				8		2	25	7					2	1			3	7			2	14		
24X,CC	219.56	56.373	33	24	237	22				1			6						6				1	3				11		

Table 1

Cibicidoides pseudoperlucidus	Cibicidoides subspiratus	Clinapertina subplanispira	Conorbina marginata	Coryphostoma midwayensis	Cyclammina cancellata	Dorothia spp.	Eouvigerina spp.	Epistominella exigua	Frondicularia jarvisi	Fursenkoina spp.	Gaudryina laevigata	Gavelinella beccariiformis	Gavelinella hyphalus	Gavelinella rubiginosa	Gavelinella velascoensis	Globimorphina sp.	Globobulimina ovata	Globocassidulina subglobosa	Glomospira gordialis	Gravellina narivaensis	Gyroidinoides acutus	Gyroidinoides depressus	Gyroidinoides girardanus	Gyroidinoides globosus	Gyroidinoides planulatus	Gyroidinoides quadratus	Gyroidinoides subangulare	Gyroidinoides vortex	Hanzawaia spp.	Haplophragmoides spp.	Heronallenia spp.	Karreriella chapapotensis	Karreriella subglabra
22										2											2				1	3							
17																		1			1											1	
																		1															
										5	2									1					2							1	
							11					7									1							1					
	8						7					3					1							1				1			1		
	1						4					9					1			3								7			1		
1						1			1			30		1			2				2	1			3	3			5				
												23					3						2		2	3			6				
						1	1					25	2				3							1	5				4				
						1	7			5		18	3				1				2	1			9				2			1	1
						1			1	8		44	2										1		7				2		2		
					1					5		122	2								2		1		3	3			1				
											2	66	9											1	13	2							
1							7			5		49	20								1				2		2	1					
	5											49	12		1	1					1				5								

Table 2

Pullenia quadriloba	Pullenia quinqueloba	Pullenia salisburyi	Pullenia subcarinata	Pyramidina rudita	Quadrimorphina allomorphinoides	Quadrimorphina profunda	Ramulina sp.	Rectobolivina carpenterae	Rheophax spp.	Rhizakina epigona	Rhizammina sp.	Siphogenerinoides brevispinosa	Spirillina vivipara	Spiroplectammina annectens	Spiroplectammina laevis	Spiroplectammina spectabilis	Stilostomella aculeata	Stilostomella annulifera	Stilostomella consobrina	Stilostomella subspinosa	Tappanina selmensis	Textularia spp.	Tritaxia aspera	Tritaxia globulifera	Tritaxia havanense	Tritaxia paleoceanica	Tritaxia pyramidata	Trochamminoides proteus	Turrilina brevispira	Turrilina robertsi	uniocular taxa	uniserial lagenids	Valvulineria camerata	Vulvulina spp.
4		1	3		1							26						5	12		47										2	4		
			2									98						3	11		79										1	6		
		1								1		72						4	5	1	72								15		1	2		
2												6						1	4		164								43		1	6		
												2							5		32								3		1	9		
3					1							5						16	38		95								2		8	15		
1						17											2	6	13		88								4		4	9		
2					1		1										3	3	20		55				1				3		6	16		
5										3							2	3	26		20								2		10	20		
4							1										4		20	3	11					2					8	20		
1																	7	2	11		9										2	26		
3							1										6	5	27		3								1		9	20		
		1	1														3	4	28		19				1						3	14		
	1									1							3	2	22		2										3	6		
1																1	4	5	10		15		3						1		2	12		
	4	3						5				1				14		3	28	5	5	2					1				2	11		
																6			12												3	3		

Appendix 2. *Faunal data, Site 6690*

sample	depth, mbsf	age, Ma	number of species	number of species (100)	number of specimens	Abyssamina poagi	Abyssamina quadrata	Alabamina creta	Allomorphina trigona	Anomalinoides acutus	Anomalinoides capitatus	Anomalinoides semicribratus	Anomalinoides spissiformis	Anomalinoides spp.	Aragonia aragonensis	Aragonia velascoensis	Bolivinoides cf. decorata	Bolivinoides delicatulus	Bolivinoides laevigatus	Bulimina macilenta	Bulimina midwayensis	Bulimina ovula	Bulimina cf. semicostata	Bulimina simplex	Bulimina thanetensis	Bulimina trinitatensis	Buliminella beaumonti	Ceratobulimina sp. small
16H-1, 41- 43	138.21	54.690	56	42	318	1			1				8				12					18		27				6
16H-2, 41- 43	139.71	54.729	57	39	326	7		1					2				6					35		14				2
16H-3, 41- 43	141.21	54.767	45	31	334	11							3				20					57	5	9		4	2	
16H-4, 41- 43	142.72	54.805	52	37	314	1	3						7	1			23					15		30		4		1
16H-5, 41- 43	144.21	54.843	58	38	321	8	3			5	1		21				9					28		15		2		1
16H-6, 41- 43	145.71	54.881	49	34	328	6	3			1			14				90					19		7	3			3
16HCC	147.50	54.926	35	27	291		2						3				80					20		46	3			1
17H-1, 40- 42	147.91	54.937	56	38	339		3		1				12				18					33		19	1	10		
17H-2, 40- 45	149.41	54.974	50	32	337		3		1				6				13					8		84	1	3		
17H-3, 40- 42	150.91	55.022	46	34	330		4		1				10				22					24		41		6		
17H-4, 41- 44	152.42	55.059	58	35	348		6				1		2		1		44		1			30		9	3	1		3
17H-5, 40- 42	153.91	55.095	51	33	313		1		1				8				5					6		8	1	1	1	5
17H-6, 40- 42	155.44	55.132	56	37	365	5	3		7				3				13					35		7		3		3
17H,CC	157.20	55.175	41	32	278		1						10				22					8		12	4			5
18H-1, 42- 44	157.63	55.185	46	29	320	2	6						9				78					26		12	2			
18H-2, 40- 42	159.11	55.221	42	28	324	1							8				5					17		18	4	11		
18H-3, 40- 42	160.61	55.257	54	37	342		3						8			3	10					27		21		10		3
18H-4, 40- 42	162.12	55.294	47	29	342	1	3						6				33					28		22		29		
18H-5, 40- 42	163.61	55.330	40	28	335	3							8				10					13		5	1	4		5
18H-6, 40- 42	165.11	55.366	30	22	344								16				33					19		5		3		1
18H,CC	166.65	55.403	30	23	289	2							16				6					22		12		7		11
19H-1, 40- 42	167.31	55.420	25	20	318	8							14									28		73		1		
19H-1, 74- 76	167.65	55.428	31	26	335	2	4						8				16					30		74		3		
19H-1,114-120	168.07	55.438	30	23	303	1	19						13			1	5					29		76		5		
19H-2, 40- 42	168.81	55.456	35	26	335	1							17	49			7					14		117	4	2	1	
19H-2, 74- 76	169.16	55.464	34	22	323	3							5	33			8					8		103		12		2
19H-2,118-124	169.58	55.474	35	24	323	8	5					1		5			1					16		71		14		
19H-3, 40- 42	170.31	55.492	34	25	305		18		2								26					20		28	10	3		
19H-3, 51- 53	170.42	55.495	40	31	311		19										12	1				35		6	10	2		
19H-3, 60- 62	170.51	55.497	33	25	313		20			2							14					43		4	15		1	
19H-3, 66- 68	170.57	55.499	37	29	334	1	27			1							16	8				52		5	16			
19H-3, 72- 74	170.63	55.500	66	46	318		19			2		4			1		5	5			5	19		26	28		1	
19H-3, 74- 76	170.65	55.501	63	43	322		1			5		1					6	2			2	7		11	43			
19H-3,115-121	171.05	55.511	71	44	302		4			1		2	5				12	2				8		9		1		
19H-4, 42- 44	171.85	55.533	64	39	324		3			1						1	22					13					1	
19H-4, 74- 76	172.16	55.542	70	47	312		1			3		2	3		1	1	3	2			2	9			9	1	5	
19H-5, 40- 42	173.31	55.573	66	46	302					1			2		1	1	2	4				5			2	19	1	
19H-5, 74- 76	173.69	55.584	60	38	338					2			1				1	11				6		45			3	
19H,CC	174.30	55.601	51	35	273		1			2			1				7				4	2		83				
20H-1, 40- 42	174.71	55.612	52	37	296					1			3				7					18		24				
20H-2, 40- 42	176.21	55.654	73	48	342								4				3	7				10		4		2	6	4
20H-3, 40- 42	177.71	55.696	65	42	307		2			3			1				5	6			1	4		27		1		
20H-4, 41- 43	179.22	55.739	61	37	343					2			1				2	3	5		12	5		61				1
20H,CC	180.28	55.768	52	34	308								1			1	6	8			1	6		25				1
21H-1, 40- 42	180.71	55.780	61	41	297	1						1					1	3			15	5		27				2
21H-2, 40- 42	182.21	55.822	67	38	334	1											6	2			1	7		7				
21H-3, 40- 42	183.71	55.864	62	44	316			1					4					5			5	4		5			1	1
21H-4, 5- 7	184.86	55.896	55	36	334								1				3	6			2	12		22				1
21H,CC	185.20	55.900	54	36	261											1	1	11			7	5		56				1
22H-1, 40- 42	185.71	55.915	61	38	323					1			6			2	26				11	9		7				
22H-2, 42- 44	187.13	55.982	56	35	330		2		1				8			2	5	11			1	4		10	4			
22H-3, 42- 44	188.63	56.070	61	40	317		1					1	1					16			7	2						
22H,CC	191.15	56.163	57	43	269								1					11	6		3	2		6	6	1		

Cibicidoides dayi	Cibicidoides pseudoperlucidus	Cibicidoides subspiratus	Clinapertina subplanispira	Conorbina marginata	Coryphostoma midwayensis	Cyclammina cancellata	Dorothia spp.	Eouvigerina spp.	Epistominella exigua	Frondicularia jarvisi	Fursenkoina spp.	Gaudryina laevigata	Gavelinella beccariiformis	Gavelinella hyphalus	Gavelinella rubiginosa	Gavelinella velascoensis	Globimorphina sp.	Globobulimina ovata	Globocassidulina subglobosa	Glomospira gordialis	Gravellina narivaensis	Gyroidinoides acutus	Gyroidinoides depressus	Gyroidinoides girardanus	Gyroidinoides globosus	Gyroidinoides planulatus	Gyroidinoides quadratus	Gyroidinoides subangulare	Gyroidinoides vortex	Hanzawaia spp.	Haplophragmoides spp.	Heronallenia spp.	Karreriella chapapotensis
										1	44																						
	5						2				15												2								2		
											13												2										
	4	1									17										1		1										
	10										8				3						1											1	
											7			1									1									3	
										4	3																					2	
	17									1	10								2				1								3	1	
											13												1										
	8										12												1								4	2	
	3								2		7					1							2								4	2	
	3										7												1										
	4									1	12							1					2									4	
	3	2									7							1			3		1			3							
											3	1						1												1			
	1										12							2		2												
	5										6							1		1		1										
	6									2	27												1										
									2		12																						
											8							2		1		1										
	5																	1				1										
								7			7															1							
								7			1							1					1								3		
								4			4												2										
								3															1										
								2			3							1					11								1		
									15		1												1										
	1							1	18		5		*2																				
								6	42																							1	
	2							16	83																2								
	1								22				10									1	2	2	2								
	1	4							22				16	1									3		1	3	2					2	
	1									2	1		4		1								3			6					1		
										1	5		5										3			4					1		
	2								4		3		6									2	1			1		2					
	3									1	3		6										2	1		6	1				1		
	2								1	1	2		8	2									3	4									
	5										3		7			1							1			4	2						
	7										2		4	1									1			2							
	6								1	7	5		15	1	1								1			6	1						2
	2	1							1	5	5		6	14	1	2		1				1	2			10					2		
	4								1		2		18			1						2	1		3	9							
	8										2		5		1								2			1	1	9					1
3	12										8		1				2						2			7					1		
		1							2				13								1		1	1	2	7	1						
	6								7		2		6	2									3		2	1		1	3				
	1									11	1		13			1										7			1				
	1										1		8			1						2			1	1	2	1					
	6								2	5	6		8	11									1			3	4						
	8												22										3			3							
	4		1			1				3			5	1					1		1	2	1			6	1	5					
	5												6	14	1		1					4				4		2				1	1

Appendix 2. *continued*

sample	depth, mbsf	age, Ma	number of species	number of species (100)	number of specimens	Karreriella subglabra	Lenticulina spp.	Neoflabellina reticulata	Neoeponides hillebrandti	Neoeponides lunata	Nonion havanense	Nonionella longicamerata	Nonionella robusta	Nuttallides umbonifera	Nuttallides truempyi	Nuttallides sp., flat	Nuttallides sp., high	Nuttallinella florealis	Oridorsalis nitidus	Oridorsalis umbonatus	Orthomorphina spp.	Osangularia navarroana	Osangularia velascoensis	polymorphinid species	pleurostomellid species	Patellina corrugata	Pseudoparrella sp.	Pseudopatellinelloides sp.	Pullenia bulloides	Pullenia coryelli
16H-1, 41-43	138.21	54.690	56	42	318	7					30			2	6	12					5	2			3	28					
16H-2, 41-43	139.71	54.729	57	39	326	7					4			23	5						6	3			2	34			2		
16H-3, 41-43	141.21	54.767	45	31	334	11					15		1	23	1						9	7			1	28					
16H-4, 41-43	142.72	54.805	52	37	314	5					12		3	3	9						13	6	6		2	14					
16H-5, 41-43	144.21	54.843	58	38	321	2				2*	15	2	3	13	19						11	5	3		2	24					
16H-6, 41-43	145.71	54.881	49	34	328	3					6	1		4	15						6	4				19		1			
16HCC	147.50	54.926	35	27	291	7					11			9	13						3	4				16					
17H-1, 40-42	147.91	54.937	56	38	339	8					19		1	28	9						12	9			1	37					
17H-2, 40-45	149.41	54.974	50	32	337	7					2		2	30	17						7	8				22		1			
17H-3, 40-42	150.91	55.022	46	34	330	2					13		11	6	19						15	7			1	38					
17H-4, 41-44	152.42	55.059	58	35	348	6					18			8	20						5	3			1	14				3	
17H-5, 40-42	153.91	55.095	51	33	313	8					16		5	8	18						4	3			1	15				1	
17H-6, 40-42	155.44	55.132	56	37	365	8					14	4	10	10	8						3	6			1	31				2	
17H,CC	157.20	55.175	41	32	278	9					15	1		21	11						11	3				18					
18H-1, 42-44	157.63	55.185	46	29	320	4					10	3		3	37						6	3			1	29					
18H-2, 40-42	159.11	55.221	42	28	324	7					15		5	3	31						10	3				18		1			
18H-3, 40-42	160.61	55.257	54	37	342	8					16	2	1	4	34						9	6			2	23			1		
18H-4, 40-42	162.12	55.294	47	29	342	9					10	1	2	2	28						3	1			1	14					
18H-5, 40-42	163.61	55.330	40	28	335	6					10	1	7	6	16						2	3			3	15					
18H-6, 40-42	165.11	55.366	30	22	344	3					2	4	3	20	22						3	3				11					
18H,CC	166.65	55.403	30	23	289	2					10		6	27	15						14	2				17					
19H-1, 40-42	167.31	55.420	25	20	318	4					11		2	13	6						12					11					
19H-1, 74-76	167.65	55.428	31	26	335	8							2	7	10						8	4				13					
19H-1,114-120	168.07	55.438	30	23	303	5					5			11	8						14					7					
19H-2, 40-42	168.81	55.456	35	26	335	7					7			4	5						4	3			1	11					
19H-2, 74-76	169.16	55.464	34	22	323	9					2			15	12							1			1	13					1
19H-2,118-124	169.58	55.474	35	24	323	7							1	4	9						2			1	4	18		1			
19H-3, 40-42	170.31	55.492	34	25	305	1							2	4				1		3	8			1	20					
19H-3, 51-53	170.42	55.495	40	31	311	2					3		6	2	3			2		3	9				17					
19H-3, 60-62	170.51	55.497	33	25	313	1					1		2	3	1					3	4			1	18					
19H-3, 66-68	170.57	55.499	37	29	334					4	2		2	3		3	2			2	5			4	8					
19H-3, 72-74	170.63	55.500	66	46	318	8	1		3	6	3		2	14	6	2				4	2			2	26					7
19H-3, 74-76	170.65	55.501	63	43	322	5	2		3	5	11			30	7	3				7	3			4	17					10
19H-3,115-121	171.05	55.511	71	44	302	1	13	1			4	16		24	9	1		1		4	1		1	12	15	1				3
19H-4, 42-44	171.85	55.533	64	39	324	7						14	6	2	29	20	1			2	3			10	10					6
19H-4, 74-76	172.16	55.542	76	47	312	11	1				3	13	1	4	24	13	10			2	4			11	13					9
19H-5, 40-42	173.31	55.573	66	46	302	9					4		5	6	7	3				2	3			9	11					12
19H-5, 74-76	173.69	55.584	60	38	338	6	1				1		11	3	14	6				2	3			11	13					6
19H,CC	174.30	55.601	51	35	273	6					1		9	13	4	3				3	1			4	7					13
20H-1, 40-42	174.71	55.612	52	37	296	7					3		6	20	6	1				1	3			9	12					1
20H-2, 40-42	176.21	55.654	73	48	342	16	1			4	1		9	1	4	14	14			3	4			7	12				2	5
20H-3, 40-42	177.71	55.696	65	42	307	6				2	3		4	3	12	24	3			3	9			3	9				1	3
20H-4, 41-43	179.22	55.739	61	37	343	5	1			2	8		6	2	27	5	6			1	1			8	7					3
20H,CC	180.28	55.768	52	34	308	12				4	7	1		21	14					6	1			2	5					2
21H-1, 40-42	180.71	55.780	61	41	297	8					5	7	2	3	18	1	10			7	1	1		2	9					9
21H-2, 40-42	182.21	55.822	67	38	334	6	3			4	8	5	3	6	21	12	15			2	3			4	8					6
21H-3, 40-42	183.71	55.864	62	44	316	23	5			4	2			33		3				1	2			4	1					18
21H-4, 5-7	184.86	55.896	55	36	334	15					3		8	1	3	16	11			5	1			9	9					6
21H,CC	185.20	55.900	54	36	261	15					9	10	3	7	4	3				2	2			5	4					1
22H-1, 40-42	185.71	55.915	61	38	323	7				1	3	1	2	11	3	9				5				5	5					3
22H-2, 42-44	187.13	55.982	56	35	330	10				1	1	8	2	3	14	4	2			1	1			9	8					5
22H-3, 42-44	188.63	56.070	61	40	317	9					3	3	2	7	22	6							1	5	3					8
22H,CC	191.15	56.163	57	43	269	20					2	6	1	15	1	8				6					10					5

Pullenia jarvisi	Pullenia quadriloba	Pullenia quinqueloba	Pullenia salisburyi	Pullenia subcarinata	Pyramidina rudita	Quadrimorphina allomorphinoides	Quadrimorphina profunda	Ramulina sp.	Rectobolivina carpenterae	Rheophax spp.	Rhizakina epigona	Rhizammina sp.	Siphogenerinoides brevispinosa	Spirillina vivipara	Spiroplectammina annectens	Spiroplectammina laevis	Spiroplectammina spectabilis	Stilostomella aculeata	Stilostomella annulifera	Stilostomella consobrina	Stilostomella subspinosa	Tappanina selmensis	Textularia spp.	Tritaxia aspera	Tritaxia globulifera	Tritaxia havanense	Tritaxia paleocoanica	Tritaxia pyramidata	Trochamminoides proteus	Turrilina brevispira	Turrilina robertsi	unilocular taxa	uniserial lagenids	Valvulineria camerata	Vulvulina spp.
	1	1					1		1			2	13					17			2	25	19						2	3	2	5	20		
		1				2			2			2	19	2				12				35	43				4	2			4	19				
	1						1					2	47					8				22	14					2	4		4	4				
1	2					2	1		1			2	20	1				27				29	24					2			5	13				
	1	1	1								1	39					18				18	5								5	13					
	3	2	4					1			1	30					38				10	7						1			6	9				
		2					1				1	10					16				13	11								2	9					
	4	1			2			2			5	12					15				8	11						3	1		8	11				
		1					3				1	24					8		23	18	6							2		11	9					
	2					3				3	26					8			5	19				1			1		4	11						
	2	1	2		1		8		2	43					8			8	54								7	12								
	2					2		1	120					4			9	31							3	12										
		3				2		2	50					5	3	11	71								6	11										
	5					7		1	13					3		19	46								4	11										
	1	2			2		1	30						25	4							2		3	13										
	1		2		6			13						21	98							1		3	5										
1	3	2	3		4			20	1			4	30	50								6	16												
	3	1	1		3		1	62	2				15	13								10	4												
1	2	3			4	1	1	114	1			10	59						1		1	5													
	1				16		76				1	9	75						5	2															
						46				5	57						1	1	2																
				5	1	94				14	7						4	4	10																
					1	87				6	20					2	5	1	9																
					1	43				6	33					2	4	1	1																
5			3		1	8				10	38						1	2	2																
			6		1				20	59						1	4																		
			29		1		6	14	78						4	2	3																	
3		1	3			7	114					4	1	7																				
	1	10		5	12	10	92					8	3	6																				
	5	11	24		22	48					11	6	4																						
	8	12	10		2	12	13					7	4	2																				
2		1	5	4	1	18		2	2	7	8	4		1	2	5	17																		
	8	1	12		1	6	19	11	4		1	6	9																						
	1	5	1	1	51	1	1	1	21	16			1	3	1	7	22																		
3	2	20		11	1	1	67	3	1	2	7	36																								
	1	1	2	1	18		58	3	2	1	5	39																								
2	1	13	1	69	1	45	2	1	1	4	28																	2								
	1	5	1	93	1	2	3	32	1	9	1	2	1	5	12																				
	1	21	2	26	12	1	1	3	19																										
11		3	6	1	49	1	42	5	2	7	30																									
3	7	1	79	3	8	2	34	5	4	3	6	14																								
5	1	1	2	79	2	2	19	4	2	5	9																									
3	1	86	1	11	1	25	3	5	11																1											
	1	2	8	95	1	16	4	1	3	22																										
2	1	2	39	37	8	2	4	24																												
	1	79	1	1	17	1	45	2	1	4	23																									
2	1	14	43	3	3	3	1	34	3	12	7	29			5																					
	28	7	1	1	103	1	4	21																												
	2	5	2	5	59	1	1	2	18																											
	1	1	73	2	1	1	9	49	1	3	1	7	15																							
	29	1	59	6	2	61	2	3	1	5	8																									
	1	83	1	11	1	8	39	1	5	1	5	27																	1							
	4	2	44	13	4	2	20	4									1	6	20																

Appendix 3. *Faunal data, Site 525*

sample	depth, mbsf	age, Ma	number of species	number of species (100)	number of specimens	Abyssamina poagi	Abyssamina quadrata	Alabamina creta	Allomorphina trigona	Anomalinoides acutus	Anomalinoides capitatus	Anomalinoides semicribratus	Anomalinoides spissiformis	Anomalinoides spp.	Aragonia aragonensis	Aragonia velascoensis	Bolivinoides cf. decorata	Bolivinoides delicatulus	Bolivinoides laevigatus	Bulimina callahani	Bulimina macilenta	Bulimina midwayensis	Bulimina ovula	Bulimina cf. semicostata	Bulimina simplex	Bulimina thanetensis	Bulimina trinitatensis	Buliminella beaumonti	Ceratobulimina sp. small
32-4, 75-77	388.86	55.383	46	35	313		12					1	2		2					3			26		66		11		
32-4,125-127	389.36	55.394	47	33	322		4						4		4					4			7		51		12	1	
32-5, 25-27	389.86	55.404	42	31	312		10						3		6		1			13		5	18	6	56				
32-5, 48-50	390.08	55.412	47	31	329		5								9		2			3			14		86		4		
32-5, 77-79	390.38	55.419	39	32	330		5						3		9		2			15			16		59		5		
32-5,115-117	390.76	55.427	34	25	309		14								42					10			17		30		1		
32-6, 25-27	391.36	55.441	52	40	350		17								34		1			13		2	17		27		10	1	
32-6, 50-52	391.61	55.447	43	32	324		20						1		29		2			6			13		18		2		
32-6, 76-78	391.87	55.454	49	35	326		9		1				7		6		5			3			13		11		17		
32-6, 90-92	392.01	55.457	53	40	313		7						4		21		4			2			13		13		11		
32-6,113-115	392.24	55.475	54	39	343		44								11		1						19		14		1	8	1
32-6,130-132	392.41	55.491	34	27	328		13								34		5						3		16		11	3	
32-6,145-147	392.56	55.501	60	40	317		37	1				1		9	10	2	1			3		9	6	7	8		1	
32-7, 22-24	392.81	55.519	81	56	352		2	2				5		6			3					1	20		3	4	1	3	
32-7, 53-55	393.11	55.540	73	52	309		4	1				8		5			3	1				3	13			5			

sample	depth, mbsf	age, Ma	number of species	number of species (100)	number of specimens	Karreriella subglabra	Lenticulina spp.	Neoflabellina reticulata	Neoeponides hillebrandti	Neoeponides lunata	Nonion havanense	Nonionella longicamerata	Nonionella robusta	Nuttallides umbonifera	Nuttallides truempyi	Nuttallides sp. flat	Nuttallides sp. high	Nuttallinella floralis	Oridorsalis nitidus	Oridorsalis umbonatus	Orthomorphina spp.	Osangularia navarroana	Osangularia velascoensis	polymorphinid species	pleurostomellid species	Patellina corrugata	Pseudoparrella sp.	Pseudoparella/linelloides sp.	Pullenia bulloides	Pullenia coryelli	Pullenia jarvisi
32-4, 75-77	388.86	55.383	46	35	313	19					8	3	5	1	28					10	2		1	1	24						
32-4,125-127	389.36	55.394	47	33	322	12					4	1			23					11	7				39						
32-5, 25-27	389.86	55.404	42	31	312	11					8			2	27					8	2			1	20						
32-5, 48-50	390.08	55.412	47	31	329	17					6		6	2	18					12	1			1	24						
32-5, 77-79	390.38	55.419	39	32	330	19					6		5	3	20					15	8			1	28						
32-5,115-117	390.76	55.427	34	25	309	12					15		6	2	50					7					12						
32-6, 25-27	391.36	55.441	52	40	350	14					7		1	2	56					1			2	1	22			1			
32-6, 50-52	391.61	55.447	43	32	324	18					14	4	4	6	38					6	1				22						
32-6, 76-78	391.87	55.454	49	35	326	13					12	2	4	1	65					10	2			2	23			1			
32-6, 90-92	392.01	55.457	53	40	313	12					15	1	6		6					9	4			1	23						
32-6,113-115	392.24	55.475	54	39	343	10					10		8		45					8	2			3	35						
32-6,130-132	392.41	55.491	34	27	328	10					4		7		108	2				17	2			1	22						
32-6,145-147	392.56	55.501	60	40	317	4			2	6	5		5		18	5	4		5	48	1		1	4	14			1		1	5
32-7, 22-24	392.81	55.519	81	56	352	12	1		1	4	4	1	8		8	2				9	2		1	7	20			1			5
32-7, 53-55	393.11	55.540	73	52	309	14	1			1	6		5		8	2	18		4	10	4			11	8						8

Table (part 1)

Cibicidoides dayi	Cibicidoides pseudoperlucidus	Cibicidoides subspiratus	Clinapertina subplanispira	Conorbina marginata	Coryphostoma midwayensis	Cyclammina cancellata	Dorothia spp.	Eouvigerina spp.	Epistominella exigua	Frondicularia jarvisi	Fursenkoina spp.	Gaudryina laevigata	Gavelinella beccariiformis	Gavelinella hyphalus	Gavelinella rubiginosa	Gavelinella velascoensis	Globimorphina sp.	Globobulimina ovata	Globocassidulina subglobosa	Glomospira gordialis	Gravelina narivaensis	Gyroidinoides acutus	Gyroidinoides depressus	Gyroidinoides girardanus	Gyroidinoides globosus	Gyroidinoides planulatus	Gyroidinoides quadratus	Gyroidinoides subangulare	Gyroidinoides vortex	Hanzawaia spp.	Haplophragmoides spp.	Heronallenia spp.	Karrenella chapapotensis
12	7										3								4				4										
12	13										5								1		1		1										
1	8										3								11				2		1	3						1	
2	3									1	6		1						4						3							1	
	11										9								11													1	
9	6										6								11			1	2		1	3							
13	16										7								22		1	1	5						1			1	
18	24										8								7				2	1								1	
18	11										3								8		3	1	2	4								1	
13	17										4								1		1	1	1										
	17									1	2								3		1	3											
2								5			1											5											
1	1			1	1							7	1						6		1	11			3	1						1	
10				9		2					9	15	2						5	5		1			5	7							
8				6		6					7	17	6						2	1	1	3	4								1	

Table (part 2)

Pullenia quadriloba	Pullenia quinqueloba	Pullenia salisburyi	Pullenia subcarinata	Pyramidina rudita	Quadrimorphina allomorphinoides	Quadrimorphina profunda	Ramulina sp.	Rectobolivina carpenteriae	Rheophax spp.	Rhezakina epigona	Rhizammina sp.	Siphogenerinoides brevispinosa	Spirillina vivipara	Spiroplectammina annectens	Spiroplectammina laevis	Spiroplectammina spectabilis	Stilostomella aculeata	Stilostomella annulifera	Stilostomella consobrina	Stilostomella subspinosa	Tappanina selmensis	Textularia spp.	Tritaxia aspera	Tritaxia globulifera	Tritaxia havanense	Tritaxia paleoceanica	Tritaxia pyramidata	Trochamminoides proteus	Turrilina brevispira	Turrilina robertsi	uniloccular taxa	uniserial lagenids	Valvulineria camerata	Vulvulina spp.
						3						10						7				2	17									3	11		
	5		2		2	1						50			1			20			11										2	12	1	
		1	2		1	2						24						15			33										2	7	1	
	2											11			1			14			52										2	13	3	
					4							18						14			29											11		
					6							20						2			20											4		
	2			1	4							12						2			18	1									2	6		
	1			1	4							28						5			7								27		1	16	1	
	3				2	7						16						7	9	3	2								19		5	10		
				3	11		1					20						5	2	5	2	26	1						5		3	17		
	2			4		1						7						1	11	26									3		1	5		
	2			1								1						1	8	31				1					7	2	3	1	
	2				1							12	1		1			2	24	21		7		5	1					9	32	3	4
	3			1	2		1					18		9	4			10	14		8			4	3					4	20	1	2

Appendix 4. *Faunal data, Site 527*

sample	depth, mbsf	age, Ma	number of species	number of species (100)	number of specimens	Abyssamina poagi	Abyssamina quadrata	Alabamina creta	Allomorphina trigona	Anomalinoides acutus	Anomalinoides capitatus	Anomalinoides semicribratus	Anomalinoides spissiformis	Anomalinoides spp.	Aragonia aragonensis	Aragonia velascoensis	Bolivinoides cf. decorata	Bolivinoides delicatulus	Bolivinoides laevigatus	Bulimina callahani	Bulimina macilenta	Bulimina midwayensis	Bulimina ovula	Bulimina cf. semicostata	Bulimina simplex	Bulimina thanetensis	Bulimina trinitatensis	Buliminella beaumonti	Ceratobulimina sp., small
24-1, 62- 64	199.63	55.504	31	24	320	20							20		2				3			14					1		
24-1, 85- 89	199.86	55.424	37	28	313	13							21				11					15	4				1		
24-1,102-104	200.03	55.433	39	27	324	20							12		8		16					20	6			2			
24-1,136-138	200.37	55.457	32	27	304	30							11		18		6					15	3						
24-2, 5- 7	200.56	55.470	31	22	315	50							26		19		15					14	6						
24-2, 20-22	200.71	55.480	19	15	342	59							20		1		2		2			29							
24-2, 38- 40	200.89	55.493	24	20	216	64							12		3		1			1		7							
24-2, 56-58	201.07	55.507	53	37	349	25	1			3		3	17		2	12				1		4				12	1	3	
24-2, 68- 70	201.19	55.519	62	41	344	10						3	3			9						2				29			
24-2, 80- 82	201.31	55.529	57	40	320	18						1	19			7						2				33		1	
24-2, 88- 90	201.39	55.538	63	42	321	7							11			7			1			1				27	1		
24-2,115-117	201.66	55.561	60	42	312	6				2		6	2		4	1	1			2						38	2		
24-3, 28- 30	202.29	55.629	55	41	332	7							5			2		1		1						53		1	
24-3, 48-50	202.49	55.646	60	42	316	2	1					1	6			6			2	1		1				33	1	2	
24-3, 75- 77	202.76	55.662	62	42	317	2						4	8			6		1								15			

sample	depth, mbsf	age, Ma	number of species	number of species (100)	number of specimens	Karreriella subglabra	Lenticulina spp.	Neoflabellina reticulata	Neoeponides hillebrandti	Neoeponides lunata	Nonion havanense	Nonionella longicamerata	Nonionella robusta	Nuttallides umbonifera	Nuttallides truempyi	Nuttallides sp. flat	Nuttallides sp. high	Nuttallinella floreallis	Oridorsalis nitidus	Oridorsalis umbonatus	Orthomorphina spp.	Osangularia navarroana	Osangularia velascoensis	polymorphinid species	pleurostomellid species	Patellina corrugata	Pseudoparrella sp.	Pseudopatellinelloides sp.	Pullenia bulloides	Pullenia coryelli	Pullenia jarvisi
24-1, 62- 64	199.63	55.504	31	24	320								15	8	65					18					39						
24-1, 85- 89	199.86	55.424	37	28	313								15	5	61					14				2	22						
24-1,102-104	200.03	55.433	39	27	324						3	1	8	12	63					7					38						
24-1,136-138	200.37	55.457	32	27	304						4		6	13	54					13	3			2	23						
24-2, 5- 7	200.56	55.470	31	22	315								11	2	51					11				2	26						
24-2, 20-22	200.71	55.480	19	15	342								5	26	67					24					1						
24-2, 38- 40	200.89	55.493	24	20	216								3	7	50	5				6					2						
24-2, 56-58	201.07	55.507	53	37	349	3			23	36	10		13		33	8	30		10	17				1	6					5	1
24-2, 68- 70	201.19	55.519	62	41	344	6			4	4	12	1	8		37	14	1		4	18	2			11	9					5	
24-2, 80- 82	201.31	55.529	57	40	320	5				6	12	7	5		35	6	9		2	4	1			7	7					2	3
24-2, 88- 90	201.39	55.538	63	42	321	7	1		2	5	8		4		28	7	4		2	6				10	6					10	
24-2,115-117	201.66	55.561	60	42	312	1			3	4	1		5		16	3	7		3	5			2	15	5					5	
24-3, 28- 30	202.29	55.629	55	41	332	7			5	5			6		28	8	4		3	10				9	6					4	
24-3, 48-50	202.49	55.646	60	42	316	3			8	12			9		14	15	6		5	1				17	8			1		2	
24-3, 75- 77	202.76	55.662	62	42	317	4	2		4	3			11		28	16			5	8				7	10					5	1

Cibicidoides dayi	Cibicidoides pseudoperlucidus	Cibicidoides subspiratus	Clinapertina subplanispira	Conorbina marginata	Conyzhostoma midwayensis	Cyclammina cancellata	Dorothia spp.	Eouvigerina spp.	Epistominella exigua	Frondicularia jarvisi	Fursenkoina spp.	Gaudryina laevigata	Gavelinella beccariiformis	Gavelinella hyphalus	Gavelinella rubiginosa	Gavelinella velascoensis	Globimorphina sp.	Globobulimina ovata	Globocassidulina subglobosa	Glomospira gordialis	Gravellina narivaensis	Gyroidinoides acutus	Gyroidinoides depressus	Gyroidinoides girardanus	Gyroidinoides globosus	Gyroidinoides planulatus	Gyroidinoides quadratus	Gyroidinoides subangulare	Gyroidinoides vortex	Hanzawaia spp.	Haplophragmoides spp.	Heronallenia spp.	Karreriella chapapotensis
	24							3			19							4					6			3							
	22							5			35							6					2			1							
	16										23		1					3		1			2			1							
	28									2	33							4								3						1	
	24										20							4	1							2							
	21									1	1							11		1						5						1	
2	16										3							3	2														2
	8						1						11	4											4	2							
	8						8						19	3										1	1	8							
	7						1				6		3					1			1	2	1		4	1							
	14	1					12				2		16	4											1	3	6	1					
	8						7						16	4		1								3	5	1							
	7						3	3			8		23	5											1	9	3						
1	5				1		5				5		17	11									5	5									
	7						7				3		22	3									2	1									

Pullenia quadriloba	Pullenia quinqueloba	Pullenia salisburyi	Pullenia subcarinata	Pyramidina nutila	Quadrimorphina allomorphinoides	Quadrimorphina profunda	Ramulina sp.	Rectobolivina carpentierae	Rheophax spp.	Rhezakina epigona	Rhizammina sp.	Siphogenerinoides brevispinosa	Spirillina vivipara	Spiroplectammina annectens	Spiroplectammina laevis	Spiroplectammina spectabilis	Stilostomella aculeata	Stilostomella annulifera	Stilostomella consobrina	Stilostomella subspinosa	Tappanina selmensis	Textularia spp.	Tritaxia aspera	Tritaxia globulifera	Tritaxia havanense	Tritaxia paleoceanica	Tritaxia pyramidata	Trochamminoides proteus	Turrilina brevispira	Turrilina robertsi	uniloculata taxa	uniserial lagenids	Valvulineria camerata	Vulvulina spp.
				2		20						5									24								1		9	1		
					2	14						3									17								2		9	5		
						12						2									27								11		4	4		
		2				11						1									9								6		3			
					4	8															11										4	4		
						34															32													
					1	20						1									2							1						
3								4			2	3					3				1		5							1	2	3		
1								17				37		1		4	6	1			1		15							2	4	13		
								23				25		4			19	1			4		2		3						8	12		
								24			1	21		3			13	1					2		10						4	18	1	
								12			3	49		12			16	1		1					11						4	10		
								7				38		4			14	4						5	8	1					6	14	1	
								5				52		5			9	2	1					1	4						8	10		
								4				45		5			13	23						4	4			2			6	19		

Appendix 5. Isotope data, Sites 689, 690, 525, 527

Site 689

sample	depth, mbsf	age, Ma	Cibicidoides spp. δ18O	Cibicidoides spp. δ13C	Bulimina spp. δ18O	Bulimina spp. δ13C	Lenticulina spp. δ18O	Lenticulina spp. δ13C	T. selmensis δ18O	T. selmensis δ13C	O. umbonatus δ18O	O. umbonatus δ13C	N. truempyi δ18O	N. truempyi δ13C	G. beccariiformis δ18O	G. beccariiformis δ13C	A. mckannai d δ18O	A. mckannai d δ13C	A. mckannai e δ18O	A. mckannai δ13C	M. convexa (d+e) δ18O	M. convexa (d+e) δ13C	bulk δ18O	bulk δ13C
22H-4, 40-42	202.41	55.380	0.12	1.41	0.26	1.02	-0.01	-0.03	0.00	0.79	0.23	0.89					-0.42	2.37	-0.44	2.32				
22H-4, 108-116	203.08	55.401	0.11	1.56	0.29	1.03	-0.08	0.12	0.26	0.69	0.34	1.04	0.24	1.17			-0.79	2.86	-0.77	2.81				
22H-5, 40-42	203.91	55.427			0.27	1.22	0.07	0.55	0.22	1.31	0.36	0.78	0.02	1.34			-0.65	3.10	-0.58	2.91				
22H-5,113-118	204.63	55.450			0.61	1.00	0.17	0.27	0.40	0.61			0.13	1.10										
22H,CC	205.43	55.475			-0.26	-0.36	0.49	-0.65	-0.98	-0.95														
23X-1, 40-42	207.61	55.490					-1.26	-1.23	-0.79	-0.65							-1.22	-0.03	-0.91	1.63	-1.55	-1.28		
23X-1,116-119	208.38	55.501					-0.29	-0.92									-1.18	0.49						
23X-2, 40-42	209.11	55.510					0.20	0.43									-0.31	2.94						
23X-3, 42-44	210.61	55.621					0.28	2.19							0.50	1.51	-0.44	3.37	-0.37	3.22				
23X-4, 40-42	212.11	55.700													0.30	1.07			0.05	3.67				
23X,CC	212.85	55.980					0.61	2.80					0.35	2.18	0.20	2.12								
24X-1, 42-44	217.33	56.242					0.24	1.66					0.23	1.81	0.54	2.16								
24X-1,112-114	218.03	56.283			0.43	1.49			0.47	1.35			-0.03	0.68	0.26	1.33								
24X,CC	219.56	56.373					0.09	0.89					0.33	1.40	0.14	0.41								

Site 690

sample	depth, mbsf	age, Ma	Cibicidoides spp. δ18O	Cibicidoides spp. δ13C	Bulimina spp. δ18O	Bulimina spp. δ13C	Lenticulina spp. δ18O	Lenticulina spp. δ13C	T. selmensis δ18O	T. selmensis δ13C	O. umbonatus δ18O	O. umbonatus δ13C	N. truempyi δ18O	N. truempyi δ13C	G. beccariiformis δ18O	G. beccariiformis δ13C	A. mckannai d δ18O	A. mckannai d δ13C	A. mckannai e δ18O	A. mckannai δ13C	M. convexa (d+e) δ18O	M. convexa (d+e) δ13C	bulk δ18O	bulk δ13C
18H-3, 40-42	160.61	55.257	-0.03	1.88	0.07	1.12	-0.24	0.53	-0.15	0.73			-0.35	1.07										
18H-4, 40-42	162.12	55.294	-0.99	2.03			-0.30	0.48					-0.04	1.82										
18H-5, 40-42	163.61	55.330							0.02	0.66			-0.38	1.26			-1.03	3.44	-1.02	3.20				
18H-6, 40-42	165.11	55.366							0.86	0.82			0.08	1.36			-0.97	3.76	-0.82	3.46				
18H,CC	166.66	55.403											0.15	1.45										
19H-1, 40-42	167.31	55.420					-0.77	-0.32					-0.34	1.17										
19H-1, 74-76	167.65	55.428					-0.67	0.39					-0.78	1.58										
19H-1,114-120	168.07	55.438					-0.91	-1.10	0.16	0.44	0.23	-0.11	-0.25	1.67										
19H-2, 40-42	168.81	55.456			0.20	0.22	-0.69	-1.38					-0.71	0.77										
19H-2, 74-76	169.16	55.464					-0.24	0.06					-0.53	0.54										
19H-2,118-124	169.58	55.475			-0.49	-0.65	-0.87	-1.89	-0.39	-1.26			-0.77	-0.03			-1.87	2.40	-1.46	2.34				
19H-3, 40-42	170.31	55.492			-0.53	-0.65	-1.45	-1.75	-0.98	-1.37			-1.39	-0.70			-1.68	0.78	-1.67	0.56	-2.15	1.23		
19H-3, 51-53	170.42	55.495															-1.60	0.07	-1.51	0.34	-1.45	1.30		
19H-3, 60-62	170.51	55.497															-1.53	0.00	-0.99	0.19				
19H-3, 66-68	170.57	55.499																						
19H-3, 72-74	170.63	55.500													0.22	1.67	-1.45	0.23	-1.23	0.52	-2.10	1.03		
19H-3, 74-76	170.65	55.501													0.09	1.11			-1.23	0.23	-2.05	1.14		
19H-3,115-121	171.05	55.511			-0.18	0.51	0.28	-0.49					0.06	1.85	0.08	1.18	0.57	3.24	-0.78	2.86				
19H-4, 42-44	171.85	55.533					0.02	0.18					0.02	1.26			-0.37	3.94	-0.10	3.61				
19H-4, 74-76	172.18	55.642					0.32	0.97			0.53	1.16	0.08	1.47					-0.54	4.82				
19H-5, 40-42	173.31	55.573					-0.35	-0.05					0.04	1.51					-0.51	4.11				
19H-5, 74-76	173.69	55.584					-0.27	-0.76					-0.08	1.61	0.33	1.56			-0.74	3.51				
19H,CC	174.30	55.601											0.06	1.51										
20H-1, 40-42	174.71	55.612	0.12	2.04			-0.28	-0.13					-0.24	2.95	0.23	1.94	0.61	4.06	-0.30	4.08				
20H-2, 40-42	176.21	55.664	0.01	2.00			-0.21	0.73					-0.16	1.89	0.23	2.84			-0.86	2.73				
20H-3, 40-42	177.71	55.696	0.23	2.39			-0.20	0.09					0.14	2.84	0.23	1.73			-0.46	4.24				
20H-4, 41-43	179.22	55.739	0.26	2.84			-0.23	0.65					0.11	2.18	0.94	2.26			-0.44	4.10				
20H,CC	180.28	55.788											0.46	2.43										
21H-1, 40-42	180.71	55.780	0.20	2.52			-0.42	-0.18					0.07	1.89					-0.59	4.15				
21H-2, 40-42	182.21	55.822											0.09	2.33	0.34	1.97			-0.65	4.15				
21H-3, 40-42	183.71	55.864	0.16	2.79									0.07	1.87	0.21	1.80			-0.70	4.22				
21H-4, 5-7	184.86	55.896					-0.06	1.47					0.01	2.08					-0.81	4.06				

Site 525

Sample	Depth	Age			
32-4, 75- 77	388.86	55.382	-0.74	0.52	-0.66	1.68
32-4,125-127	389.36	55.394	-0.37	1.19	-0.05	1.78
32-5, 25- 27	389.86	55.404	-0.34	1.07	0.60	1.16
32-5, 48- 50	390.08	55.412	-0.28	0.98		
32-5, 77- 79	390.38	55.419	-0.37	1.09	-0.57	1.81
32-5,115-117	390.76	55.427	-0.03	1.15	-0.53	1.82
32-6, 25- 27	391.36	55.441	-0.26	0.96	-0.73	1.86
32-6, 50- 52	391.61	55.447	-0.52	0.88	-0.74	1.55
32-6, 76- 78	391.87	55.454	-0.30	1.10	-0.74	1.79
32-6, 90- 92	392.01	55.457	-0.29	1.09	-0.73	1.94
32-6,113-115	392.24	55.475	-1.06	-1.09	-1.26	0.45
32-6,130-132	392.41	55.491	-1.50	-1.47	-1.80	-0.07
32-6,145-147	392.56	55.501	-0.93	-0.03	-1.76	0.47
32-7, 22- 24	392.81	55.519	0.03	1.27	-0.77	2.05
32-7, 53-55	393.11	55.540	-0.32	1.53	-0.73	2.40

Site 527

Sample	Depth	Age			
24-1, 62- 64	199.63	55.404	-0.14	0.82	-0.59	1.80
24-1, 85- 89	199.86	55.424	-0.11	0.76	-0.41	1.76
24-1,102-104	200.03	55.433	-0.32	0.65	-0.57	1.70
24-1,136-138	200.37	55.457	-0.45	0.29	-0.51	1.43
24-2, 5- 7	200.56	55.470	-0.67	-0.18	-0.65	1.29
24-2, 20-22	200.71	55.480	-1.35	-0.98	-1.56	0.34
24-2, 38- 40	200.89	55.493	-1.36	-0.92	-1.04	0.23
24-2, 56-58	201.07	55.507	-0.32	1.12	-0.90	2.13
24-2, 68- 70	201.19	55.519	-0.74	1.00	-0.88	2.10
24-2, 80- 82	201.31	55.529	-0.32	1.23	-0.77	2.01
24-2, 88- 90	201.39	55.538	-0.22	1.40	-0.70	2.37
24-2,115-117	201.86	55.561	-0.03	1.42	-0.57	2.39
24-3, 28- 30	202.29	55.629	-0.07	1.30	-0.58	2.49
24-3, 48-50	202.49	55.646	-0.37	1.15	-0.65	2.55
24-3, 75- 77	202.76	55.662	-0.16	1.25	-0.62	2.55